



Article

Hydrogen Production from Sugarcane Bagasse Pentose Liquor Fermentation Using Different Food/Microorganism and Carbon/Nitrogen Ratios under Mesophilic and Thermophilic Conditions

Luísa Mattiello-Francisco ¹, Filipe Vasconcelos Ferreira ² , Guilherme Peixoto ^{2,3}, Gustavo Mockaitis ^{1,2} and Marcelo Zaiat ^{2,*}

¹ Interdisciplinary Research Group on Biotechnology Applied to Agriculture and the Environment (GBMA), School of Agricultural Engineering (FEAGRI), University of Campinas (UNICAMP), Av. Candido Rondon, 501—University City, São Paulo 13083-875, Brazil; lumfrancisco@gmail.com (L.M.-F.); gusmock@unicamp.br (G.M.)

² Laboratory of Biological Processes, Center for Research, Development and Innovation in Environmental Engineering, São Carlos School of Engineering, University of São Paulo, 1100, João Dagnone Ave., Santa Angelina, São Carlos 13563-120, Brazil; filipevasconcelos@usp.br (F.V.F.); guilherme.peixoto@unesp.br (G.P.)

³ Department of Bioprocesses and Biotechnology, Faculty of Pharmaceutical Sciences, São Paulo State University (FCFAR/UNESP), Araraquara—Jaú Road, Km 1, Araraquara 14801-902, Brazil

* Correspondence: zaiat@sc.usp.br



Citation: Mattiello-Francisco, L.; Ferreira, F.V.; Peixoto, G.; Mockaitis, G.; Zaiat, M. Hydrogen Production from Sugarcane Bagasse Pentose Liquor Fermentation Using Different Food/Microorganism and Carbon/Nitrogen Ratios under Mesophilic and Thermophilic Conditions. *Fermentation* **2024**, *10*, 432. <https://doi.org/10.3390/fermentation10080432>

Academic Editor: Jishi Zhang

Received: 28 May 2024

Revised: 10 July 2024

Accepted: 30 July 2024

Published: 18 August 2024



Copyright: © 2024 by the authors. Licensee MDPI, Basel, Switzerland. This article is an open access article distributed under the terms and conditions of the Creative Commons Attribution (CC BY) license (<https://creativecommons.org/licenses/by/4.0/>).

Abstract: Hydrogen is a well-known clean energy carrier with a high energetic yield. Its versatility allows it to be produced in diverse ways, including biologically. Specifically, dark fermentation takes advantage of organic wastes, such as agro-industrial residues, to obtain hydrogen. One of these harmful wastes that is poorly discharged into streams is sugarcane bagasse pentose liquor (SBPL). The present study aimed to investigate hydrogen generation from SBPL fermentation in batch reactors by applying different food/microorganism (2–10 F/M) and carbon/nitrogen (10–200 C/N) ratios under mesophilic and thermophilic conditions. Biohydrogen was produced in all pentose liquor experiments along with other soluble microbial products (SMPs): volatile fatty acids (VFAs) (at least 1.38 g L⁻¹ and 1.84 g L⁻¹ by the average of C/N and F/M conditions, respectively) and alcohols (at least 0.67 g L⁻¹ and 0.325 g L⁻¹ by the average of C/N and F/M conditions, respectively). Thermophilic pentose liquor reactors (t-PLRs) showed the highest H₂ production (H₂ maximum: 1.9 ± 0.06 L in 100 C/N) and hydrogen yield (HY) (1.9 ± 0.54 moles of H₂ moles of substrate⁻¹ in 2 F/M) when compared to mesophilic ones (m-PLRs). The main VFA produced was acetate (>0.85 g L⁻¹, considering the average of both nutritional conditions), especially through the butyrate pathway, which was the most common metabolic route of experimental essays. Considering the level of acid dilution used in the pretreatment of bagasse (H₂SO₄ (1%), 1.1 atm, 120 °C, 60 min), it is unlikely that toxic compounds such as furan derivatives, phenol-like substances (neither was measured), and acetate (<1.0 g L⁻¹) hinder the H₂ production in the pentose liquor reactors (PLRs). Sugarcane bagasse pentose liquor fermentation may become a suitable gateway to convert a highly polluting waste into a renewable feedstock through valuable hydrogen production.

Keywords: hydrogen; pentose liquor; xylose; sugarcane bagasse; batch reactors; mesophilic condition; thermophilic condition; F/M ratios; C/N ratios

1. Introduction

The continuing depletion of fuel reserves and the steady rise of environmental awareness are two major reasons for seeking alternative and sustainable energy sources. Hydrogen emerges as one of the most interesting candidates as it generates water after its

combustion since its molecular backbone has no carbon, sulfur, or nitrogen included, showing a high energy yield of 122 kJ g^{-1} [1], which is 2.75 times greater than regular fossil fuels [2]. To date, total H_2 production comes almost exclusively from reforming fossil fuels (natural gas, oils, and coal) [3]. As H_2 has become an important energy source, its production and distribution encompass concepts of ecological sustainability (especially during its production stage).

Among the various forms of obtaining hydrogen, the biological way is likely the most environmentally friendly as it achieves two goals at once: Commonly associated with anaerobic digestion, it gives a final destination for hard-degradation residues that have no clear safe disposal, and it produces biofuel, which has potential energetic and economic assets [4,5]. Dark fermentation (DF) is a feasible technology when considering cost efficiency. A large range of feeds can be managed by DF, often including organic wastes [6,7].

The biohydrogen generated through DF can be obtained by adopting mesophilic and thermophilic conditions. The evaluation of optimum temperature ranges for hydrogen production is complex because it involves multiple parameters (pH, type of inoculum, residue characteristics, and reactor configuration) that interfere with the overall process. In general, thermophilic temperatures are more favorable for hydrogen production as they reduce the probable development of H_2 consumers in microbiota reactors, enhance enzymatic reaction rates, and thereafter boost the hydrolysis of solid particles [8–11]. Some of these possible explanations were brought to light by [11] when the authors reported higher HY ($0.81 \text{ molH}_2 \text{ molglucose}^{-1}$) in thermophilic fermentation than in mesophilic conditions ($0.47 \text{ molH}_2 \text{ molglucose}^{-1}$) using cheese whey powder as raw material. The thermophilic condition was also more favorable for higher hydrogen production than the mesophilic condition, as indicated in [12]. This study adopted hydrolyzed wheat as a substrate in one of its experimental conditions, and it had the highest cumulative production (752 mL) and the highest HY ($2.40 \text{ molH}_2 \text{ molglucose}^{-1}$) at 55°C . Hot temperatures (70 – 80°C) ease the H_2 transference from the liquid to gas phase, reducing the inhibitory effect for H_2 producers caused by high H_2 partial pressure in liquid media. Thus, at high temperatures, reactors could contain a greater amount of H_2 , with pressure values above 2000 Pa [13,14]. On the other hand, mesophilic conditions have no energetic demands for heating, which substantially reduces the operational cost. In addition to cost benefits, running the system under mild temperature conditions does not face some of the disadvantages encountered under harsh temperature conditions, such as poor efficiency in effluent removal, dewatering of residual sludge, and operation complexity in achieving two objectives, namely H_2 production during thermophilic fermentation and wastewater depuration [15].

There are other operational parameters that also affect H_2 production, such as carbon/nitrogen (C/N) and food/microorganism (F/M) ratios. They are usually analyzed to enhance clarification processes in wastewater treatments. However, there is also a large number of scientific papers that evaluated C/N and F/M ratios and their effect on H_2 production using different substrates [5,16–18]. Optimum values of C/N and F/M ratios for biohydrogen production have been exhibited with great variability over different studies: For instance, a study found C/N = 47:1 using anaerobic sewage sludge as the seed and sucrose as the substrate in batch reactors [19], whereas C/N was 100:2.2 in anaerobic sequencing batch reactors (ASBRs) used for the fermentation of cassava wastewater [20]. In another study, the authors determined F/M = 7–10 to be optimal when they evaluated the effect of F/M ratios (1–10) on H_2 production using anaerobic sludge in batch reactors filled with mixed food as substrate under two different temperatures: 35 and 50°C [16]. Lastly, F/M = 0.5–1.0 was evaluated in a study in which the authors aimed to investigate the effect of several parameters (initial pH, initial pH combined with F/M ratio, different types of seed, and the initial pH applied in substrate pretreatment) on the H_2 yield using complex biomass waste [4]. This shows a strong interrelation between these operational parameters with a reactor configuration and/or physicochemical characteristics of a specific substrate.

No matter which temperature conditions are adopted for hydrogen production, a feasible feedstock should be chosen that encompasses energetic, environmental, and economic aspects. Lignocellulose residues from agroindustry activities are well suited considering the above-mentioned features. They are available in large amounts, they are inexpensive, and they show energetic potential [21–23]. The molecular structure is made up of 5- and 6-carbon sugar polymers that act as fermentable sugars. Sugarcane bagasse is one of the most abundant lignocellulosic residues produced worldwide, mostly in tropical countries. Nowadays, around 50% of sugarcane bagasse is stockpiled [24,25], representing a notable risk of self-combustion and a waste of potential energy resources. In Brazil (mainly in São Paulo state) over the last decades, environmental legislation against traditional land burning practices before harvesting has been enforced [26], leading to restraint in throwing away even more bagasse residues which could have been taken advantage of as energetic feedstock.

Second-generation bioethanol production uses sugarcane bagasse as lignocellulosic core material. After a pretreatment stage (commonly steam explosion or diluted acid treatment) that breaks down hemicellulose structure into pentose and hexose monomers, softening the cellulose molecule to ease enzymatic hydrolysis attack, a xylose-rich hydrolysate is produced. As the usual 6-carbon sugar fermenter yeast *Saccharomyces cerevisiae* is not able to deal with 5-carbon sugars [27] and the genetically modified pentose fermenting microorganisms are highly priced and yield poorly under ordinary hexose fermentation, sugarcane bagasse pentose liquor (SBPL) is often discharged into streams without suitable wastewater treatment. It is a concerning pollutant in virtue of its high chemical oxygen demand (COD) concentration and recalcitrant features: above 1500 mgCOD L⁻¹ (calculated from simulated data of pentose liquor stream in a biorefinery concept) [27], impurities as free alkali and sulfates and other remaining components comprising lignin, hemicellulose, sugar, and organic acids [28]. To avoid environmental issues and to generate newly revenues in refineries from SBPL, the authors in [27] evaluated economically simulated scenarios of 1G and 2G integrated bioethanol refinery concepts. Some propositions would take advantage of pentose sugars extracted from pretreatment of lignocellulose portion to produce biogas or butanol. As basal operations defined for all scenarios (503 tonnes of sugarcane stalks per hour in 167 days of operation, 122 kg of bagasse per dry stalk, 5% of bagasse stockpiled for boilers, and 58 dry tonnes of bagasse per hour available for biorefinery), the schemes that produced biogas or butanol from pentose liquor obtained, at least, an Internal Rate Return (IRR) of 11%.

Regarding the dark fermentation hydrogen from the SBPL, most studies were accomplished on a lab scale pursuing the optimization of H₂ production using the observation of operational parameters such as the type of pretreatment of bagasse (biological, physical, chemical), or the usage of more than one method combined [29–32], the kind of inoculum [30,33–35], mineral supplementation [36], etc. To date, there is no operational biorefinery on an industrial scale conceptualized to generate hydrogen from xylose-rich liquor of sugarcane bagasse. The main bottlenecks to be overcome regarding the production of added value byproducts (such as hydrogen, organic acids, butanol, acetone) from SBPL in 2G biorefinery lie in obtaining cost-effective and greener pretreatments for the sugarcane bagasse [37] and pentose sugar fermentation with high yield and low-cost at large scale [38].

The present study aimed at producing biohydrogen using different C/N and F/M ratios in batch reactors under thermophilic and mesophilic conditions. In addition, through this work, we aimed to contribute new insights into biofuel production using unconventional agro-industrial residues, such as SBPL.

2. Methods

2.1. Overall Procedure for H₂ Production

H₂ production was carried out in 2 L batch reactors (Duran[®] flasks, DWK Life Sciences GmbH, Wertheim, Germany) with a reactional volume of 1 L at different temperatures (30 and 55 °C). Under both mesophilic and thermophilic conditions (represented here by

codes “m” and “t”, respectively) the same experiments were carried out: in the first round, the F/M ratio was verified, whilst in the second, different C/N ratios were tested. All reactors were maintained under constant agitation in reciprocating shakers (100 min^{-1}) with an initial pH of 6.0 over 35 days. The autoclaved nutritional media (described further in another topic) were injected with N_2 gas for 10 min to keep an anaerobic environment. The main carbon source came from xylose obtained from pentose liquor (almost 85% of the liquid content comprised xylose). For comparative purposes, blank samples of pure xylose (Sigma-Aldrich®, Merck KGaA, Darmstadt, Germany) were used. In the first round, different F/M ratios were applied to reactors with varying organic matter loadings ($1000\text{--}20,000\text{ mgO}_2\text{ L}^{-1}$), fixing biomass concentration at the same time (500 mgSVT^{-1}). Thus, the F/M ratios were 2, 10, 20, and $40\text{ mgO}_2\text{ L}^{-1}\text{ mgTVS}^{-1}$ corresponding to FMI, FMII, FMIII, and FMIV conditions, respectively. In the second round, different C/N ratios were applied to reactors (10, 50, 100, and 200 mgC mgN^{-1} matched to CNI, CNII, CNIII, and CNIV conditions, respectively). To meet these ratios, the nitrogen source was fixed by applying $93.5\text{ mg of CH}_4\text{N}_2\text{O L}^{-1}$ (urea) in xylose reactors (xrs) and 5.1 mg in pentose liquor reactors (plrs). The same feeding procedure adopted in the first round was also adopted in the second round.

2.2. Composition of Substrate

Organic matter loadings were measured in terms of COD. The xrs showed xylose concentrations of 935, 4673, 9346, and $18,692\text{ mg L}^{-1}$ for FM/CNI, FM/CNII, FM/CNIII, and FM/CNIV conditions, respectively. The COD values of plrs were measured after extraction of 5-carbon rich liquor. It was obtained from sugarcane bagasse adopting a procedure adapted from a previous study [39]. Briefly, the experimental extraction consisted of lignocellulose material hydrolysis with diluted acid (a H_2SO_4 solution (1% *v/v*)) applied onto dry bagasse (1:9 *w/w*). The heterogeneous solution was autoclaved under 1.1 atm, at $120\text{ }^{\circ}\text{C}$ for 60 min. The mixture was filtered for separation of the solid/liquid phases. The hydrolysate showed $13,825\text{ mg total sugars L}^{-1}$, accounting for $25,000\text{ mg O}_2\text{ L}^{-1}$ in terms of COD and a nitrogen concentration of 80 mgTKN L^{-1} , where TKN means total Kjeldahl nitrogen. Thus, to reach the desirable COD concentrations under the FM/CNI, FM/CNII, FM/CNIII, and FM/CNIV conditions, the hydrolysate was poured into reactors in amounts of 40, 200, 400, and 800 mL, respectively. As previously mentioned, nitrogen sources for both types of reactors (xrs and plrs) were obtained by adding urea. The minimum salt solution was applied to flasks according to [40]: $\text{NiSO}_4\cdot6\text{H}_2\text{O}$ (0.5 mg L^{-1}), $\text{FeSO}_4\cdot7\text{H}_2\text{O}$ (2.5 mg L^{-1}), $\text{FeCl}_3\cdot6\text{H}_2\text{O}$ (0.25 mg L^{-1}), $\text{CoCl}_2\cdot6\text{H}_2\text{O}$ (0.04 mg L^{-1}), $\text{CaCl}_2\cdot6\text{H}_2\text{O}$ (2.06 mg L^{-1}), SeO_2 (0.14 mg L^{-1}), KH_2PO_4 (5.36 mg L^{-1}), K_2HPO_4 (1.30 mg L^{-1}), and Na_2HPO_4 (2.70 mg L^{-1}). As the pentose liquor registered a low pH (<3.0), bicarbonate salt was added to adjust the initial pH to 6.0.

2.3. Inoculum

All reactors received a pre-treated inoculum from a poultry slaughterhouse UASB reactor from Dacar Industrial S.A, hosted in Tietê, São Paulo, Brazil. The steps for pretreatment of the sludge consisted of macerating and pouring a concentrated HCl solution until reaching pH 3.0 at room temperature, keeping the solution still for 24 h. Afterward, a NaOH solution was added until reaching pH 6.0 and it was kept for 48 h at room temperature. The main objective of this procedure was to inhibit the H_2 consumer microorganisms.

2.4. Monitoring Analyses

The COD, pH, and sulfate parameters were measured according to Standard Methods [41]. The total sugars were measured according to [42].

Biogas measurements (CH_4 , CO_2 , N_2 and H_2) were carried out by gas chromatography using Shimadzu® GC equipment (Shimadzu Corporation, Kyoto, Japan) with a Carboxen® 1010 (Merck KGaA, Darmstadt, Germany) ($30\text{ m} \times 0.53\text{ mm} \times 0.30\text{ }\mu\text{m}$) capillary column, and thermal conductivity detector (TCD) with argon as effluent and synthetic com-

pressed air as make-up at a 12 mL min^{-1} rate. The injector and detector worked at 220 and 230°C , respectively. The oven was programmed with an initial temperature of 40°C for 2 min; it was increased to 60°C at a rate of 5°C min^{-1} , then heated until 95°C at a rate of $25^\circ\text{C min}^{-1}$. This temperature was maintained throughout the analysis (5 min). The volume of injected biogas was $30 \mu\text{L}$.

The ideal gas equation was used for biogas volume measurements expressed under normal temperature and pressure (NTP) conditions. The variations in biogas pressure were measured using a digital manometer. The cumulative pressure was adopted by equalizing the internal flask pressure to atmospheric pressure after each measurement of the biogas pressure. The calculations of equivalent gas volume and volumetric gas rate can be observed in Equations (1) and (2), respectively.

$$V_{T\alpha} = \left(\frac{PV_H}{T} \frac{T_{CNTP}}{P_{CNTP}} \right) x_\alpha \quad (1)$$

$V_{T\alpha}$: total volume of equivalent gas α under NTP (L); P : absolute pressure of headspace (atm); V_H : volume of headspace (L); T : temperature (K); T_{CNTP} : temperature under NTP (273°K); P_{CNTP} : pressure under NTP (1 atm); x_α : gas fraction, where $\alpha = \text{H}_2, \text{N}_2, \text{CO}_2$, and CH_4 .

$$\Gamma_\alpha = \sum_{i=0}^n V_{T\alpha}^{i+1} - V_H^i \cdot x_\alpha^i \quad (2)$$

Γ_α : equivalent gas α volumetric rate (L).

Volatile fatty acid (VFA) concentrations were measured by liquid chromatography using a modular Shimadzu® chromatograph (Shimadzu Corporation, Kyoto, Japan) with a pumper system (LC-10AD), oven (CTO-20A), controller (SCL-10A), and photodiode array detector (PDA) that was adjusted to read wavelengths from 190 to 370 nm (UV spectra) at 1 nm steps, as described by [43]. The fixed phase was formed by a BIO-RAD Aminex HPX-87H (Bio-Rad Laboratories, Hercules, CA, USA) $3000 \times 7.8\text{-mm}$ column at a constant temperature of 55°C . The eluent consisted of $100 \mu\text{L}$ of the 0.005 mol L^{-1} H_2SO_4 at a 0.8 mL min^{-1} rate.

Concentration measurements of different alcohols such as ethanol, methanol, n-butanol were performed with a Shimadzu® GC2010 headspace gas chromatograph. The flame ionization detector (FID) was maintained at 280°C and fed with a mixture of H_2 and synthetic air at 30 and 300 mL min^{-1} , respectively. A Hewlett-Packard INNOWAX® column (Agilent Technologies Inc., Santa Clara, CA, USA) with a $30 \text{ m} \times 0.25 \text{ mm}$ and $0.25 \mu\text{m}$ film thickness and an H_2 flow rate of 1.6 mL min^{-1} (the same as the mobile phase) was used. The injector was maintained at 250°C with an oven temperature of 35°C . The temperature was increased at a rate of 2°C min^{-1} until a temperature of 38°C . Then, the rate was increased to $10^\circ\text{C min}^{-1}$ until reaching 75°C . Then, a rate of 2°C min^{-1} was adopted until reaching 120°C . Finally, the flux was increased to $10^\circ\text{C min}^{-1}$ until a temperature of 170°C was obtained. N_2 was used as the make-up gas (to sweep components through the detector to minimize band broadening) at a flow rate of 30 mL min^{-1} . Sample preparation was carried out by adding 1 g of NaCl , $70 \mu\text{L}$ of 1 g L^{-1} isobutanol solution (as an internal standard), and $200 \mu\text{L}$ of 2 mol L^{-1} H_2SO_4 solution into 2 mL volume. The sample flask was heated for 13 min at 100°C , and $400 \mu\text{L}$ of the sample headspace was injected with a syringe heated at 100°C [44].

2.5. Kinetic Analysis

The present study adopted a residual first-order model for a kinetic approach due to low substrate concentrations visualized in the experimental tests. This kinetic model originated through Monod's model simplification as described by [43] (Equation (3)).

$$C(t) = C_R + (C_I - C_R) \cdot e^{-k_1^{app} \cdot t} \quad (3)$$

$C(t)$: xylose concentration (mg L^{-1}); C_R : residual xylose concentration (mg L^{-1}); C_I : initial xylose concentration (mg L^{-1}); t : time(hours); k_1^{app} : apparent kinetic constant (h^{-1}). Thus, the absolute efficiency (E_a) was calculated as follows (Equation (4)):

$$E_a = 1 - \frac{C_R}{C_I} \quad (4)$$

The accumulated hydrogen production was verified using a simple dose-response sigmoidal model as shown in Equation (5).

$$H(t) = \frac{H_{\text{máx}}}{1 + 10^{(l-t) \cdot p}} \quad (5)$$

$H(t)$: accumulated H_2 production at time t (L); $H_{\text{máx}}$: maximum H_2 production (L); l : time to achieve the maximum H_2 production rate (h); p : average H_2 production rate at exponential phase (L h^{-1}).

The kinetic parameters were adjusted with the Levenberg–Marquadt algorithm using Microcal Origin® v 8.1 software (OriginLab Corporation, Northampton, MA, USA).

2.6. Statistical Analysis

Hydrogen yield (HY) measured in terms of moles of H_2 per moles of substrate was statistically compared among all experimental conditions by the ANOVA one-way test (F -value with $p = 0.05$). Regarding temperature evaluation, HY pairwise comparisons between mesophilic and thermophilic temperatures with the same F/M or C/N ratios were carried out using the Tukey test ($p = 0.05$).

3. Results

H_2 and CO_2 production took place throughout the fermentative process varying between 500 and 2000 h (21–83 days), depending on which experimental condition was observed (Figure 1). Large numbers of mpls did not fit the sigmoidal dose–response model for H_2 production, thus their production rates (p) with tpls (Table 1) could not be compared. Most experimental conditions (except the mxr-FMIII that showed the same value of txr-FMIII) reported greater H_2 production rates (HPRs) at mesophilic temperature than thermophilic ones when we compared the same F/M or C/N by turn (Table 1). In terms of the volume of H_2 produced (L), the thermophilic conditions showed higher hydrogen production compared to their pairwise mesophilic conditions (except for mxr-FMI, mxr-FMII, and mxr-FMIV which showed higher values). Even if these mesophilic conditions had reported higher volumes of hydrogen than txr-FMI, txr-FMIII, and txr-FMIV, it is worth noting that txr-FMIII and txr-FMIV showed higher HYs compared to their similar mesophilic versions from mxrs—1.0 and 0.9 mol H_2 mol S^{-1} (or 165.72 and 156 mL H_2 gSubstrate $^{-1}$), respectively.

Mxr-FMIV (0.005 L h^{-1}), mxr-CNII (0.018 L h^{-1}), and mxr-CNIII (0.003 L h^{-1}) reported greater values of H_2 productivity compared to txr-FMIV (0.002 L h^{-1}), txr-CNII (0.003 L h^{-1}), and txr-CNIII (0.002 L h^{-1}), respectively (Table 1). Interestingly, these mesophilic experimental conditions showed lower HYs compared to thermophilic equivalents (txr-FMIV, txr-CNII, and txr-CNIII): 0.84 to 0.9 (141.52 to 156 mL H_2 gSubstrate $^{-1}$), 0.7 to 1.2 (94.71 to 165.97 mL H_2 gSubstrate $^{-1}$), and 0.64 to 1.4 mol H_2 mol S^{-1} (84.54 to 185.70 mL H_2 gSubstrate $^{-1}$), respectively.

We decided to do inter and intra group comparisons with HY values (explained below). The following abbreviations will appear in the next paragraph: “F” stands for “F-value”; the first term inside parenthesis represents the degree of freedom; the second term is the total number of samples analyzed; and “prob” is the calculated α -value, i.e., the significance value of the test.

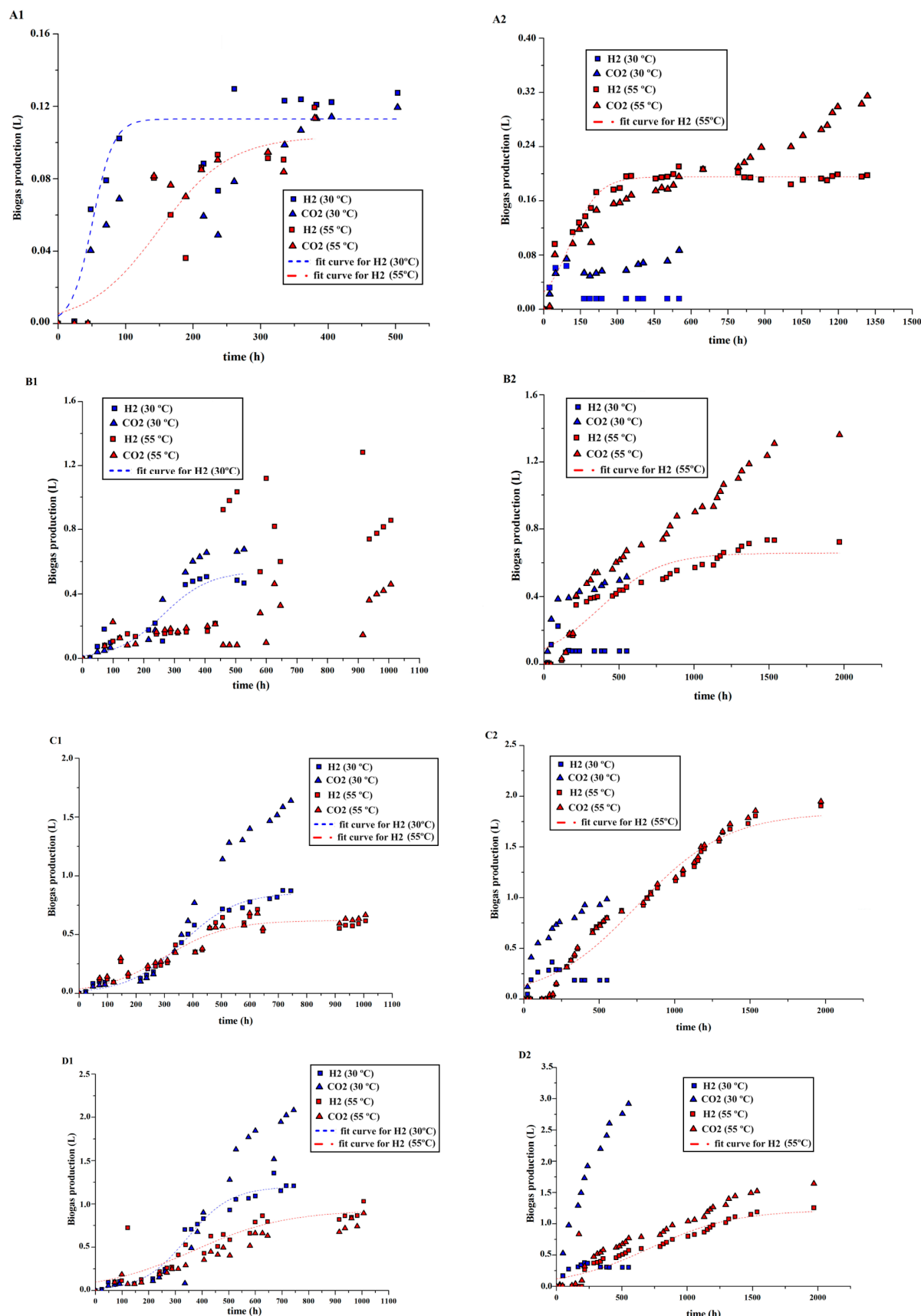


Figure 1. Cont.

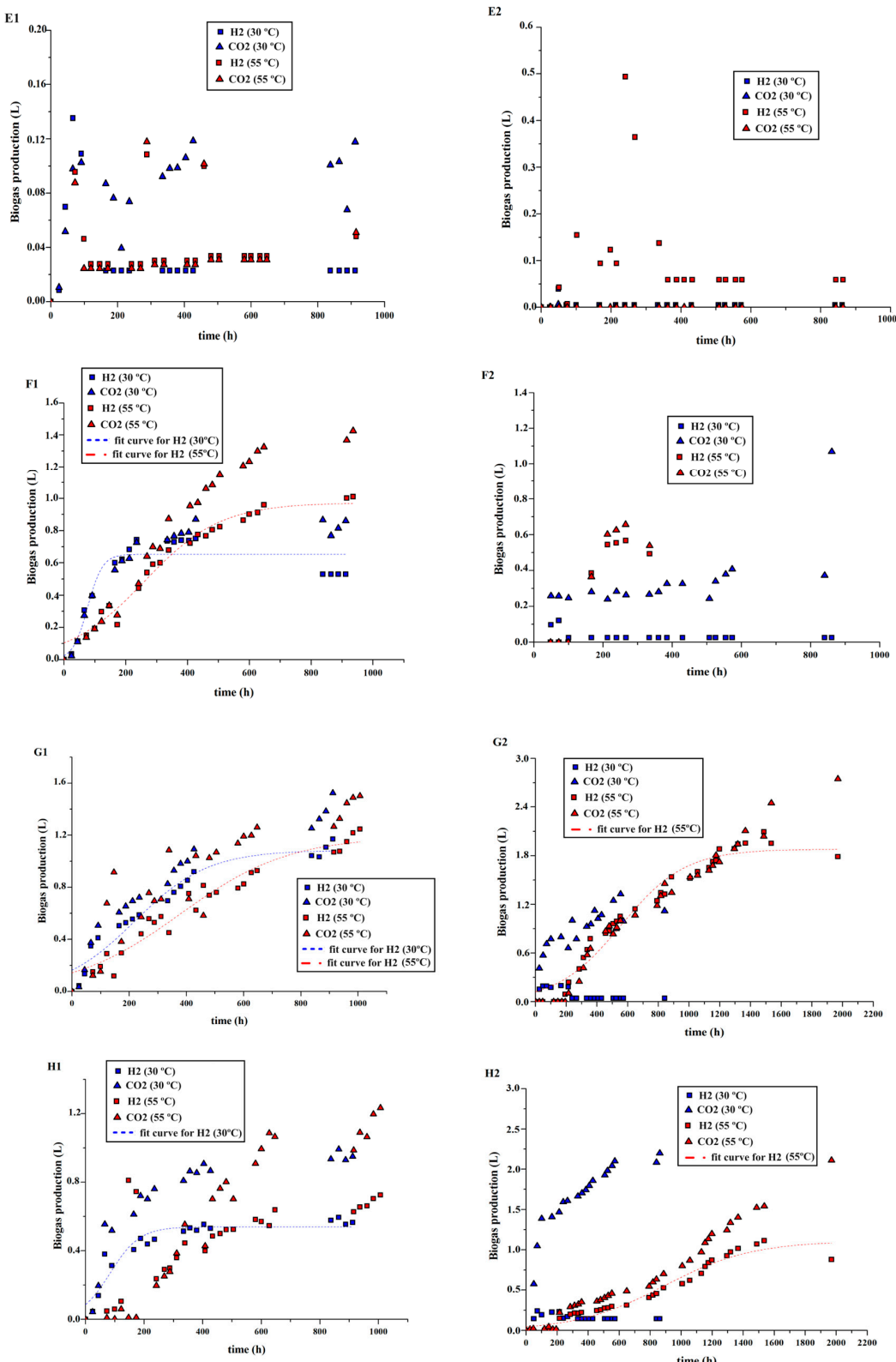


Figure 1. Biogas production at both temperatures (30 and 55 °C). Letters indicate specific F/M or C/N ratio: FMI (A1,A2); FMII (B1,B2); FMIII (C1,C2); FMIV (D1,D2); CNI (E1,E2); CNII (F1,F2); CNIII (G1,G2); CNIV (H1,H2). Numbers stand for different reactor types: xylose (1) and pentose liquor (2). The mesophilic temperature (30 °C) is depicted in blue and the thermophilic temperature (55 °C) in red.

Table 1. Kinetic parameters of substrate degradation and biogas production.

Reactor	Condition	Kinetic Parameters of Substrate					Kinetic Parameters of Biogas Production					
		k_1^{app} (h^{-1})	C_I (mg L^{-1})	C_R (mg L^{-1})	E_A	R^2	H_{\max} (L)	I (h)	p (L h^{-1})	R^2	HY^{ii} (molH_2 molS^{-1})	CO_2 (L)
mxr	F/M I	0.02 ± 0.003	1101.1 ± 76.7	1.3 ± 28	0.99	0.95	0.11 ± 0.006	52 ± 7.9	0.029 ± 0.013	0.83	0.61 ± 0.21	0.12
	F/M II	0.006 ± 0.0007	4355 ± 283.5	0.0 ⁱ	1.00	0.93	0.54 ± 0.07	262.3 ± 33.9	0.006 ± 0.002	0.85	0.85 ± 0.48	0.68
	F/M III	0.004 ± 0.0005	10,789.5 ± 750.1	0.0 ⁱ	1.00	0.89	0.86 ± 0.02	360.9 ± 9.7	0.004 ± 0.0004	0.99	0.35 ± 0.14	1.6
	F/M IV	-	-	-	-	-	1.2 ± 0.04	342.8 ± 12	0.005 ± 0.0007	0.97	0.84 ± 0.37	2.1
mplr	F/M I	0.02 ± 0.002	692.5 ± 31.9	0.0 ⁱ	1.00	0.98	-	-	-	-	0.36 ± 0.33	0.09
	F/M II	0.02 ± 0.003	3313.3 ± 223.3	0.0 ⁱ	1.00	0.95	-	-	-	-	0.22 ± 0.09	0.52
	F/M III	0.01 ± 0.002	5553.4 ± 308.2	265 ± 134.9	1.00	0.96	-	-	-	-	0.31 ± 0.11	0.98
	F/M IV	0.01 ± 0.001	10,183 ± 284.1	206.7 ± 161.7	1.00	0.99	-	-	-	-	0.22 ± 0.07	2.9
txr	F/M I	0.016 ± 0.004	1658.27 ± 140	82 ± 69.4	1.00	0.93	0.10 ± 0.014	149.2 ± 27.6	0.008 ± 0.004	0.80	0.24 ± 0.16	0.11
	F/M II	0.001 ± 0.0001	5330.4 ± 171.5	0.0 ⁱ	1.00	0.90	-	-	-	-	1.4 ± 0.72	0.46
	F/M III	-	-	-	-	-	0.62 ± 0.029	301 ± 22.5	0.004 ± 0.0007	0.89	1.0 ± 0.28	0.67
	F/M IV	-	-	-	-	-	0.93 ± 0.083	369.9 ± 49.8	0.002 ± 0.0006	0.79	0.9 ± 0.44	0.89
tplr	F/M I	0.03 ± 0.005	642.5 ± 47.5	49.4 ± 11.3	1.00	0.90	0.20 ± 0.003	109 ± 8.6	0.008 ± 0.001	0.93	1.9 ± 0.54	0.31
	F/M II	0.005 ± 0.0006	3164.8 ± 207	0.0 ⁱ	1.00	0.91	0.66 ± 0.024	367.2 ± 33	0.002 ± 0.0003	0.90	0.82 ± 0.32	1.4
	F/M III	0.001 ± 0.00001	5067.4 ± 24.2	0.0 ⁱ	1.00	0.99	1.83 ± 0.098	749.5 ± 49.7	0.001 ± 0.0001	0.95	0.99 ± 0.62	2.0
	F/M IV	-	-	-	-	-	1.2 ± 0.10	713.5 ± 86	0.001 ± 0.0004	0.93	0.78 ± 0.48	1.6
mxr	C/N I	0.022 ± 0.003	1620 ± 117.8	78.9 ± 33.7	1.00	0.92	-	-	-	-	0.18 ± 0.13	0.12
	C/N II	0.012 ± 0.001	6548.9 ± 364.5	0.0 ⁱ	1.00	0.96	0.65 ± 0.02	76.5 ± 9.3	0.018 ± 0.007	0.88	0.70 ± 0.15	0.86
	C/N III	0.003 ± 0.0003	11,167.5 ± 662.4	1753.1 ± 571	1.00	0.92	1.1 ± 0.04	220.1 ± 20	0.003 ± 0.0004	0.94	0.64 ± 0.12	1.5
	C/N IV	-	-	-	-	-	0.54 ± 0.02	83.6 ± 12.9	0.009 ± 0.002	0.89	0.52 ± 0.16	0.95
mplr	C/N I	-	-	-	-	-	-	-	-	-	0.12 ± 0.08	0.0
	C/N II	0.03 ± 0.001	4677.9 ± 76.1	124.1 ± 20.2	1.00	0.99	-	-	-	-	0.06 ± 0.04	1.1
	C/N III	0.02 ± 0.003	5026.2 ± 294.8	310.8 ± 80.8	1.00	0.94	-	-	-	-	0.13 ± 0.11	1.1
	C/N IV	0.019 ± 0.003	10,892 ± 833.9	577.3 ± 236	1.00	0.90	-	-	-	-	0.12 ± 0.03	2.2

Table 1. *Cont.*

Reactor	Condition	Kinetic Parameters of Substrate				Kinetic Parameters of Biogas Production						
		k_l^{app} (h^{-1})	C_I (mg L^{-1})	C_R (mg L^{-1})	E_A	R^2	H_{max} (L)	l (h)	p (L h^{-1})	R^2	HY^{ii} (mol H_2 mol S^{-1})	CO_2 (L)
txr	C/N I	0.02 ± 0.0004	935.6 ± 7.2	4.25 ± 1.8	1.00	1.00	-	-	-	-	0.31 ± 0.15	0.05
	C/N II	0.004 ± 0.0006	5369.7 ± 287.3	0.0^{i}	1.00	0.95	0.97 ± 0.03	260.2 ± 12.2	0.003 ± 0.0003	0.97	1.2 ± 0.18	1.4
	C/N III	-	-	-	-	-	1.2 ± 0.05	378.4 ± 27	0.002 ± 0.0003	0.95	1.4 ± 0.41	1.5
	C/N IV	-	-	-	-	-	-	-	-	-	0.75 ± 0.34	1.2
tplr	C/N I	0.01 ± 0.001	531.1 ± 27.7	0.0^{i}	1.00	0.96	-	-	-	-	1.6 ± 1.1	0.00
	C/N II	0.01 ± 0.002	4473.9 ± 305.2	0.0^{i}	1.00	0.96	-	-	-	-	0.38 ± 0.38	0.54
	C/N III	0.002 ± 0.0002	5308 ± 285	0.0^{i}	1.00	0.83	1.9 ± 0.06	555.4 ± 28.9	0.002 ± 0.0002	0.96	1.4 ± 0.76	2.8
	C/N IV	-	-	-	-	-	1.1 ± 0.06	890.1 ± 48.9	0.001 ± 0.0001	0.96	0.56 ± 0.33	2.1

ⁱ Fixed parameters to adjust to significant values in kinetic models. ⁱⁱ HYs (in terms of $\text{mL H}_2 \text{ gSubstrate}^{-1}$): mxr-FMI: 84.04 ± 33.38 ; mxr-FMII: 115.09 ± 63.25 ; mxr-FMIII: 45.98 ± 21.99 ; mxr-FMIV: 141.52 ± 75.91 ; mplr-FMI: 40.35 ± 28.62 ; mplr-FMII: 27.90 ± 10.27 ; mplr-FMIII: 42.75 ± 16.68 ; mplr-FMIV: 29.32 ± 9.99 ; txr-FMI: 36.31 ± 24.54 ; txr-FMII: 203.08 ± 108.22 ; txr-FMIII: 156.29 ± 46.26 ; txr-FMIV: 165.72 ± 109.05 ; tplr-FMI: 283.73 ± 86.73 ; tplr-FMII: 110.08 ± 52.62 ; tplr-FMIII: 143.22 ± 94.40 ; tplr-FMIV: 150.68 ± 104.72 ; mxr-CNI: 24.72 ± 16.65 ; mxr-CNII: 94.71 ± 29.59 ; mxr-CNIII: 84.54 ± 24.56 ; mxr-CNIV: 79.79 ± 27.24 ; mplr-CNI: 15.98 ± 8.02 ; mplr-CNII: 7.86 ± 4.60 ; mplr-CNIII: 19.35 ± 15.11 ; mplr-CNIV: 16.48 ± 4.01 ; txr-CNI: 44.46 ± 21.30 ; txr-CNII: 165.97 ± 25.66 ; txr-CNIII: 185.70 ± 48.84 ; txr-CNIV: 130.11 ± 62.51 ; tplr-CNI: 223.97 ± 160.22 ; tplr-CNII: 51.20 ± 56.88 ; tplr-CNIII: 206.78 ± 120.17 ; tplr-CNIV: 112.45 ± 73.22 .

The HY values throughout F/M ratios within the mxrs, txrs, and tpls groups showed significant differences, statistically speaking: $F(3;59) = 4.34$, prob = 0.008; $F(3;69) = 8.57$, prob = 6.5×10^{-5} ; and $F(3;82) = 19.65$, prob = 1.08×10^{-9} , respectively. The HYs within the mpls group were not significantly different ($F(3;44) = 1.26$, prob = 0.3). When the evaluation focused on temperature conditions between mxrs and txrs equivalents (same F/M ratio) using the Tukey Test, only the FMIII condition showed a significant difference (qvalue = 6.49, prob = 2.73×10^{-4}). Meanwhile, the pairwise comparisons between mpls and tpls, (the pentose liquor reactors) reported differences under all conditions: mpls-FMI \times tpls-FMI showed qvalue = 12.96 and prob = 4.16×10^{-8} ; mpls-FMII \times tpls-FMII showed qvalue = 4.97 and prob = 0.01; mpls-FMIII \times tpls-FMIII showed qvalue = 5.62 and prob = 0.003; and mpls-FMIV \times tpls-FMIV showed qvalue = 4.70 and prob = 0.025 (remembering in this study, the standardized α -value was $p = 0.05$).

The results throughout the C/N ratios recorded significant differences in HYs within each group constituted by mxrs, txrs, and tpls: $F(3;64) = 38.69$, prob = 2.2×10^{-14} ; $F(3;85) = 29.54$, prob = 3.50×10^{-13} ; $F(3;73) = 6.05$, prob = 9.71×10^{-4} , respectively. No statistical differences were reported within the mpls using different C/N conditions: $F(3;70) = 1.65$, prob = 0.18. The C/N ratio pairwise comparisons based on temperature conditions between the xrs and plrs apparently showed no clear tendency in relation to HY results. Considering the xrs, two comparisons were statistically different: mxr-CNII \times txr-CNII (qvalue = 6.93, prob = 6.6×10^{-5}) and mxr-CNIII \times txr-CNIII (qvalue = 9.71, prob = 3.83×10^{-8}). On the other hand, the mxr-FMI \times txr-FMI (qvalue = 1.64, prob = 0.94) and mxr-CNIV \times txr-CNIV (qvalue = 3.18, prob = 0.33) were not significantly different. In plrs, there were also two comparisons which were significantly different (mpls-CNI \times tpls-CNI (qvalue = 8.70, prob = 2.29×10^{-7}) and mpls-CNIII \times tpls-CNIII (qvalue = 8.26, prob = 9.4×10^{-7})). Meanwhile, the mpls-CNII \times tpls-CNII (qvalue = 1.69, prob = 0.93) and mpls-FMIV \times tpls-FMIV (qvalue = 2.81, prob = 0.49) were statistically equivalent.

In general, the HYs were higher at thermophilic temperature than mesophilic temperature, considering the same F/M or C/N ratio comparison. The highest cumulative H_2 production was observed at the mxrs versus txrs and at the tpls versus mpls when analyzing F/M ratios. In the case of C/N samples, higher cumulative H_2 production was found at the txrs compared with the mxrs, and at the tpls than when compared with mpls, evaluating C/N ratios. Figure 1 shows higher lag phase periods under mesophilic conditions compared to thermophilic flasks within the same nutritional ratio spectrum. The lag phase range values experienced variations due to substrate concentrations (in terms of 5-carbon amount) at both temperatures.

Within addition to H_2 production, volatile fatty acids (VFAs) and alcohols were produced throughout the dark fermentation period in all reactors (Figure 2). Acetate, butyrate, and ethanol (EtOH) are the main soluble microbial products (SMPs) (Table 2) generated in most H_2 fermentation processes, thus some parameters such as Hbu (butyric acid)/SMP_{total}, Hac (acetic acid)/SMP_{total}, EtOH/SMP_{total}, Hbu/Hac, and Hbu/EtOH were measured to better understand the fermentative liquid bulk of substances produced in the reactors (Table 3). Ethanol plus acetate dominated the SMP production over the mxr-FMI-IV conditions (Figure 2), showing EtOH/SMP_{total} of 0.26, 0.39, 0.50, and 0.51 in mxr-FMI, mxr-FMII, mxr-FMIII, and mxr-FMIV, respectively (Table 3). The acetate comprised around 10% of the total SMPs produced in these conditions. However, the mxr-FMI, the mxr-FMII, mxr-FMIII, and mxr-FMIV had an EtOH/SMP_{total} above 0.30. The sum of acetate and ethanol in these reactors represented around 60% of total SMPs produced, indicating ethanol-type fermentation. Knowing that Hbu/Hac is one of the most common parameters used to evaluate H_2 production stability in fermentation media, the highest value ratio in each of the mxr-FMs (1.65 in mxr-FMII), mpls-FMs (0.78 in mpls-FMI), tpls-FMs (0.81 in tpls-FMI), and txr-CN (0.81 in txr-CNIII) matched up with the highest HYs of each reactor group: 0.85 (115.09 $mL H_2 g Substrate^{-1}$) in mxr-FMII, 0.36 (40.35 $mL H_2 g Substrate^{-1}$) in mpls-FMI, 1.9 (283.73 $mL H_2 g Substrate^{-1}$) in tpls-FMI, and

1.4 mol H₂ mol S⁻¹ (185.70 mL H₂ gSubstrate⁻¹) in txr-CNIII. This correlation was not observed in other reactor groups, such as txr-FMs, mxr-CNs, mplr-CNs, and tplr-CNs. However, within the mxr-CNs and mplr-CNs groupings, the values of the highest HYs and the highest Hbu/Hac ratios were quite close.

Propionic acid (Hp) production peaked after 300 h (12.5 days) of fermentation under mplr-FMIV conditions, which was the second most produced SMP until the end of acidogenesis (Figure 2). This reactor showed low HY with 0.22 moles H₂ moles xylose⁻¹ (29.33 mL H₂ gSubstrate⁻¹). Mostly, mplrs had the lowest HYs along with the highest levels of propionate.

In addition to the above-mentioned SMPs, other substances such as lactate are highlighted in terms of production. Lactic acid (Hlac) became one of the main SMPs that was largely found at thermophilic temperatures, particularly in the txr-FMI, txr-FMII, txr-FMIV, and txr-CNIV conditions, accounting for 49, 43, 23, and 25% of the total SMPs, respectively.

Other VFAs with considerable production at least in one condition were isobutyric (Hib), valeric (Hva), and caproic acids (Hca). The Hib in the txr-FMIV reached values close to 100 mg L⁻¹ at the end of the fermentation process (Figure 2). The Hva showed high production under some operational conditions: the mplr-FMI reached its maximum concentration of 160 mg L⁻¹ after 500 h (20.83 days), the mplr-FMII peaked around 250 mg L⁻¹ after 300 h, and the mplr-FMIV achieved nearly 300 mg L⁻¹ after 400 h (16.7 days) (Figure 2). Finally, the Hca showed a constant production around 250 mg L⁻¹ in the mplr-FMII at 100 h (4.17 days).

Considerable concentrations of methanol (MeOH) were observed under mplr-FMII (381.89 mg COD L⁻¹), mplr-FMIII (921 mg COD L⁻¹), mxr-CNII (215.23 mg COD L⁻¹), mxr-CNIII (1261.75 mg COD L⁻¹), mxr-CNIV (2845.25 mg COD L⁻¹), mplr-CNII (981.62 mg COD L⁻¹), mplr-CNIII (430.98 mg COD L⁻¹), and mplr-CNIV (1300.96 mg COD L⁻¹) conditions (Table 2). Their concentrations accounted for 17, 24, 12, 42, 65, 41, 24, and 36% of the total SMPs produced during fermentation, respectively.

Almost total fructose degradation before total xylose consumption under mplr-FMI, mplr-FMII, mplr-FMIII, mxr-FMIII, and tplr-CNII conditions were observed probably due to initial lower fructose concentrations compared to xylose (Figure 3). In the present study, a possible strong substrate inhibition in mxr-CNIV (19.9 g L⁻¹ of xylose), txr-CNIV (18.7 g L⁻¹ of xylose), txr-FMIV (19.8 g L⁻¹ of xylose), tplr-FMIV (8.2 g L⁻¹ of xylose), and tplr-CNIV (9.8 g L⁻¹ of xylose) was verified as shown in Figure 3.

Overall, the pairwise comparison of reactors between mild and high temperatures fixing the same substrate, C/N and F/M ratios, and mesophilic environment showed higher values of k_1^{app} than thermophilic conditions (Table 1). This behavior can be related to greater SMP production at 30 °C when compared to 55 °C as shown in Table 2. Some lower kinetic parameter values also showed the highest HYs. The following conditions agreed with the last statement: txr-CNII (0.004 h⁻¹; 1.2 mol H₂ mol xylose⁻¹ or 165.97 mL H₂ g xylose⁻¹), mxr-CNII (0.012 h⁻¹; 0.70 mol H₂ mol xylose⁻¹ or 94.71 mL H₂ g xylose⁻¹), txr-FMII (0.001 h⁻¹; 1.4 mol H₂ mol xylose⁻¹ or 203.08 mL H₂ g xylose⁻¹), and tplr-CNIII (0.002 h⁻¹; 1.4 mol H₂ mol xylose⁻¹ or 206.78 mL H₂ g xylose⁻¹). Moreover, greater substrate degradations were observed in the plrs when compared to their similar xrs in terms of nutritional requirements (same F/M or C/N ratio) at both temperatures.

It is worth noting that some experimental conditions (mainly thermophilic ones) did not fit the modified Monod model as predicted in the present work.

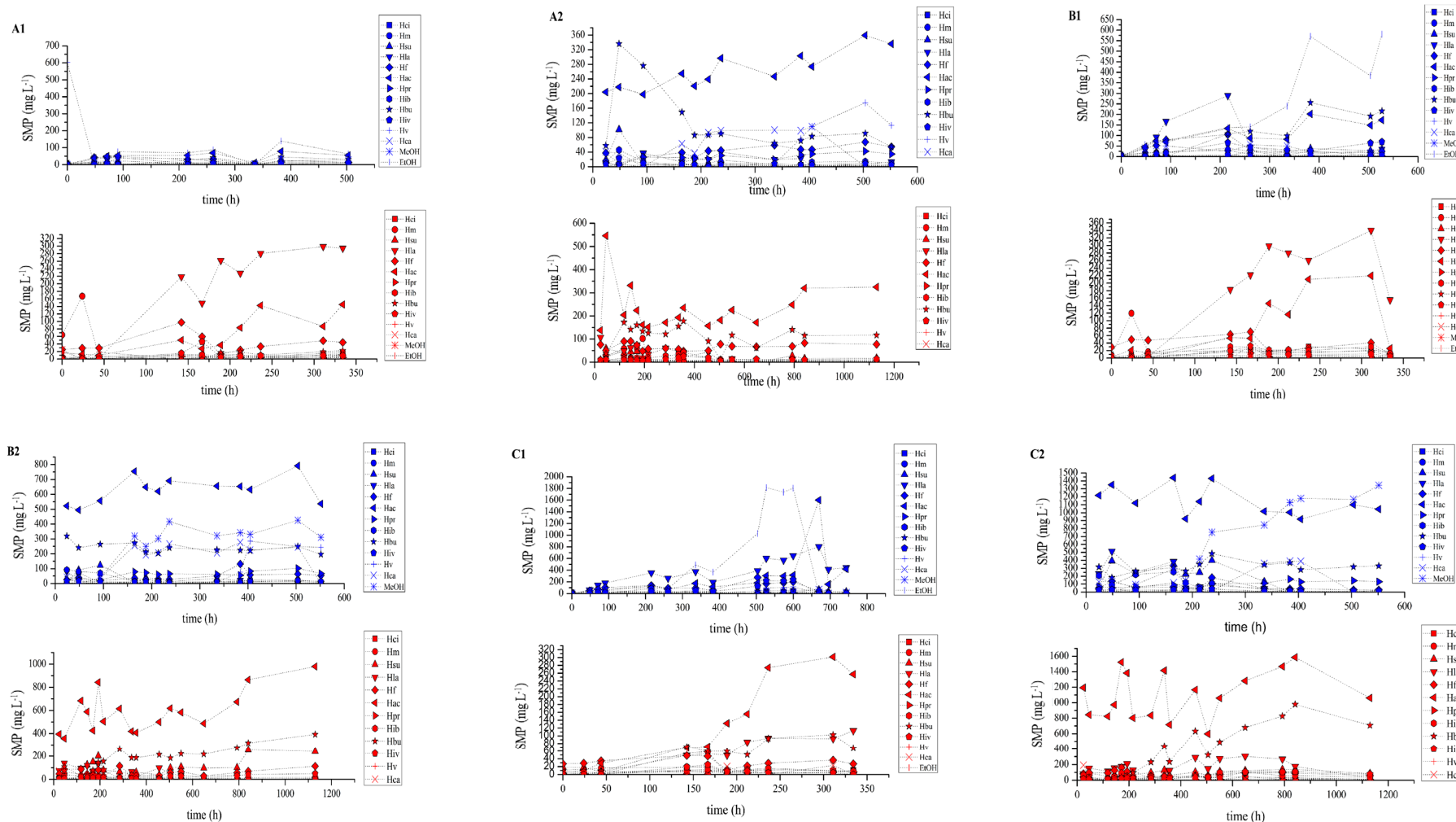


Figure 2. Cont.

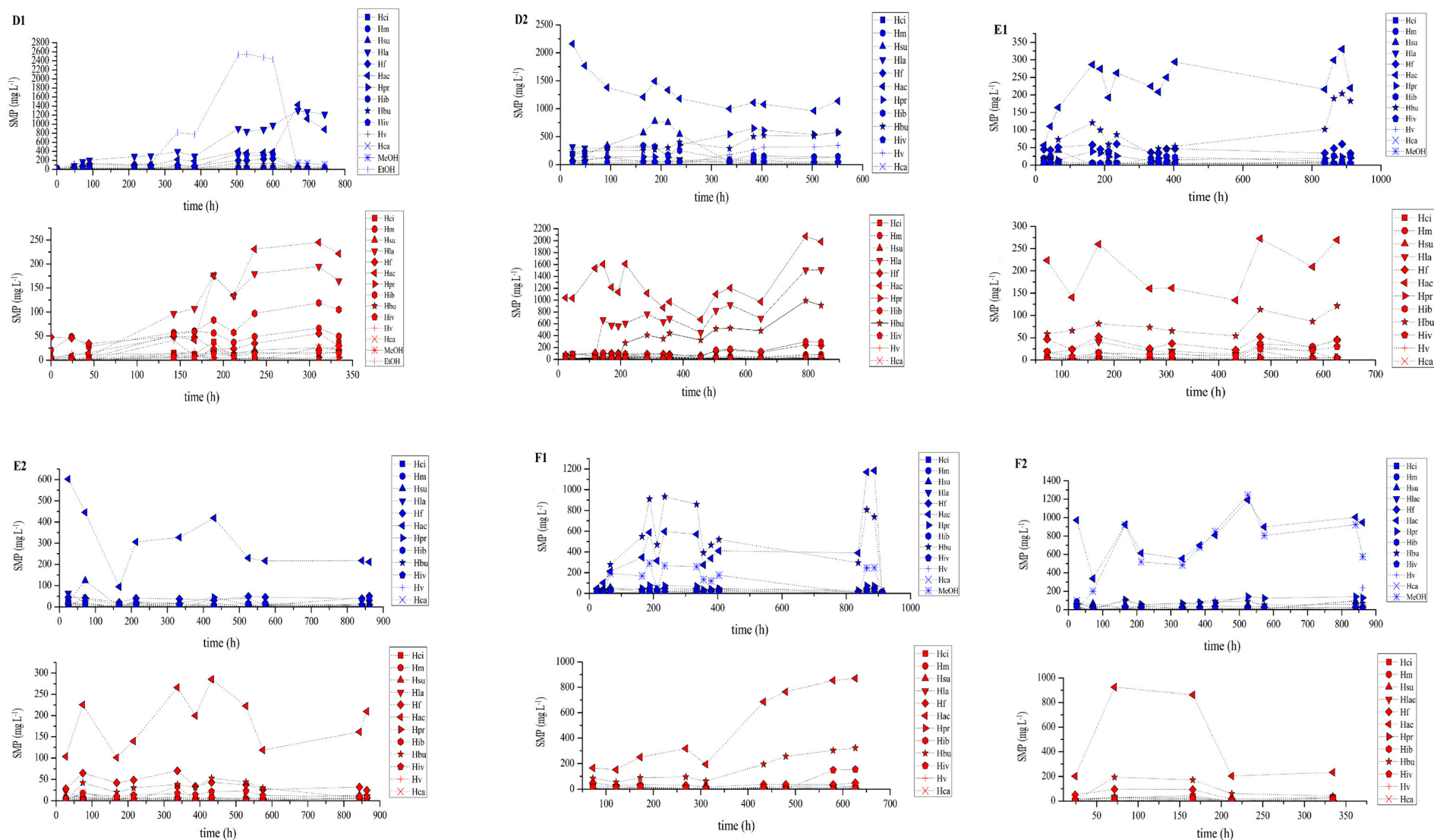


Figure 2. Cont.

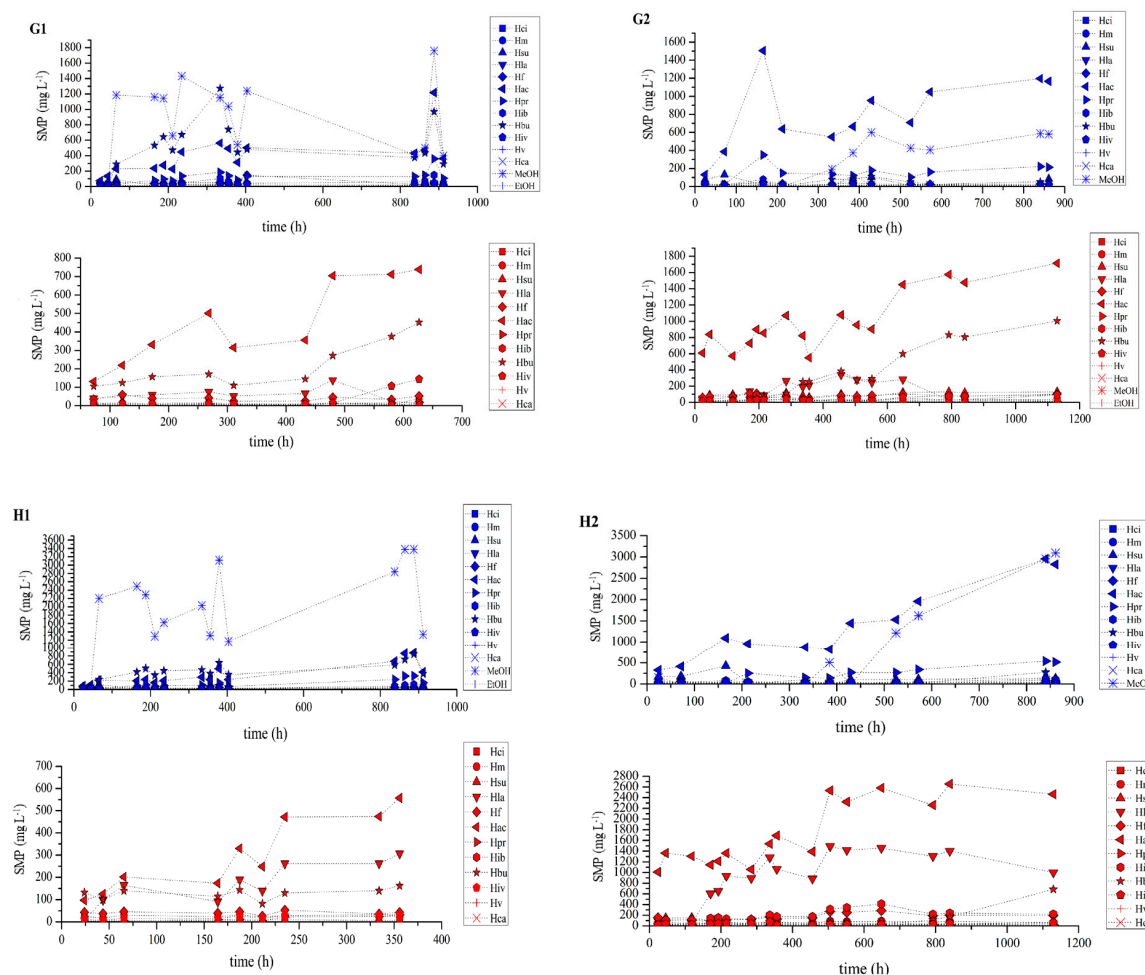


Figure 2. Soluble microbial production at both temperatures (30 and 55 °C). Letters indicate specific F/M or C/N ratio: FMI (A1,A2); FMII (B1,B2); FMIII (C1,C2); FMIV (D1,D2); CNI (E1,E2); CNII (F1,F2); CNIII (G1,G2); and CNIV (H1,H2). Numbers correspond to reactor types: xylose (1) and pentose liquor (2). Geometric forms are in blue and the mesophilic (30 °C) and thermophilic (55 °C) temperatures are in red, respectively. Hci: citric acid; Hm: malic acid; Hsu: succinic acid; Hla: lactic acid; Hf: formic acid; Hac: acetic acid; Hpr: propionic acid; Hib: isobutyric acid; Hbu: butyric acid; Hiv: isovaleric acid; Hv: valeric acid; Hca: caproic acid; MeOH: methanol; EtOH: ethanol.

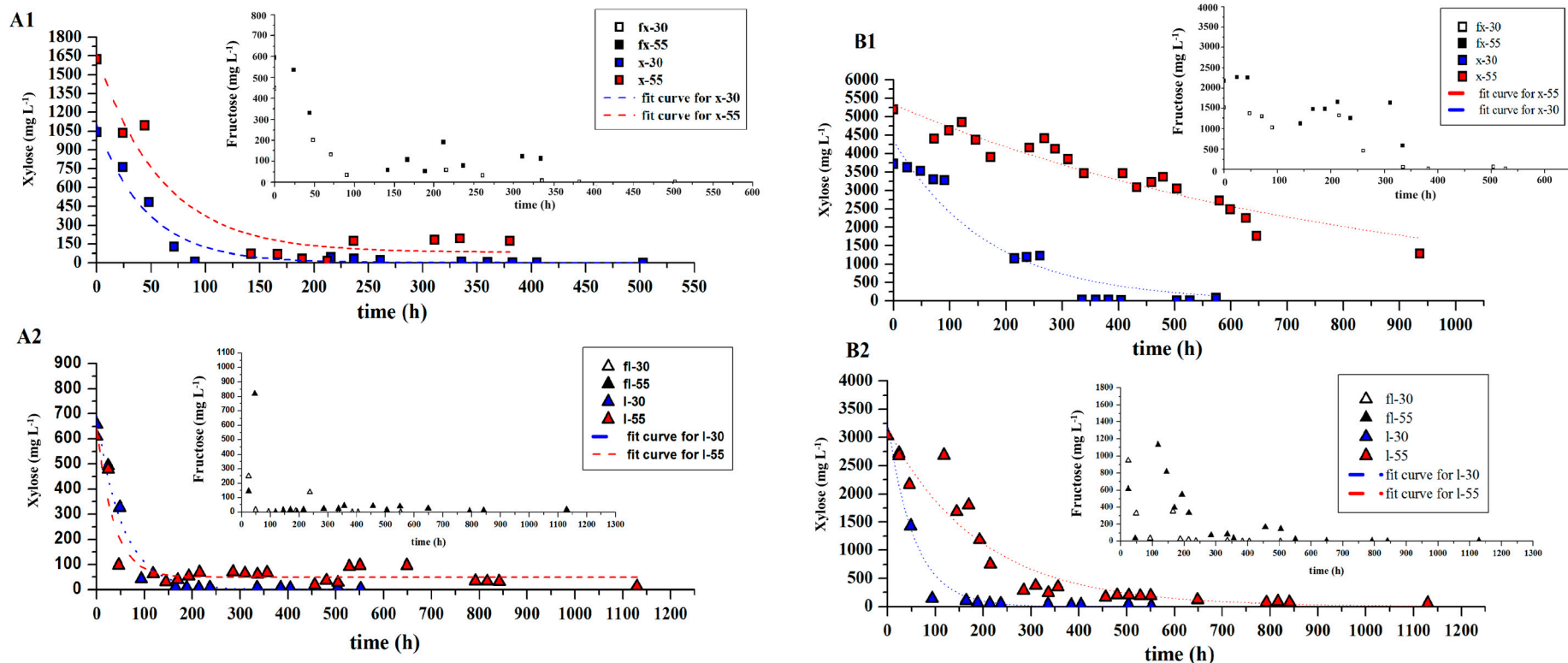


Figure 3. Cont.

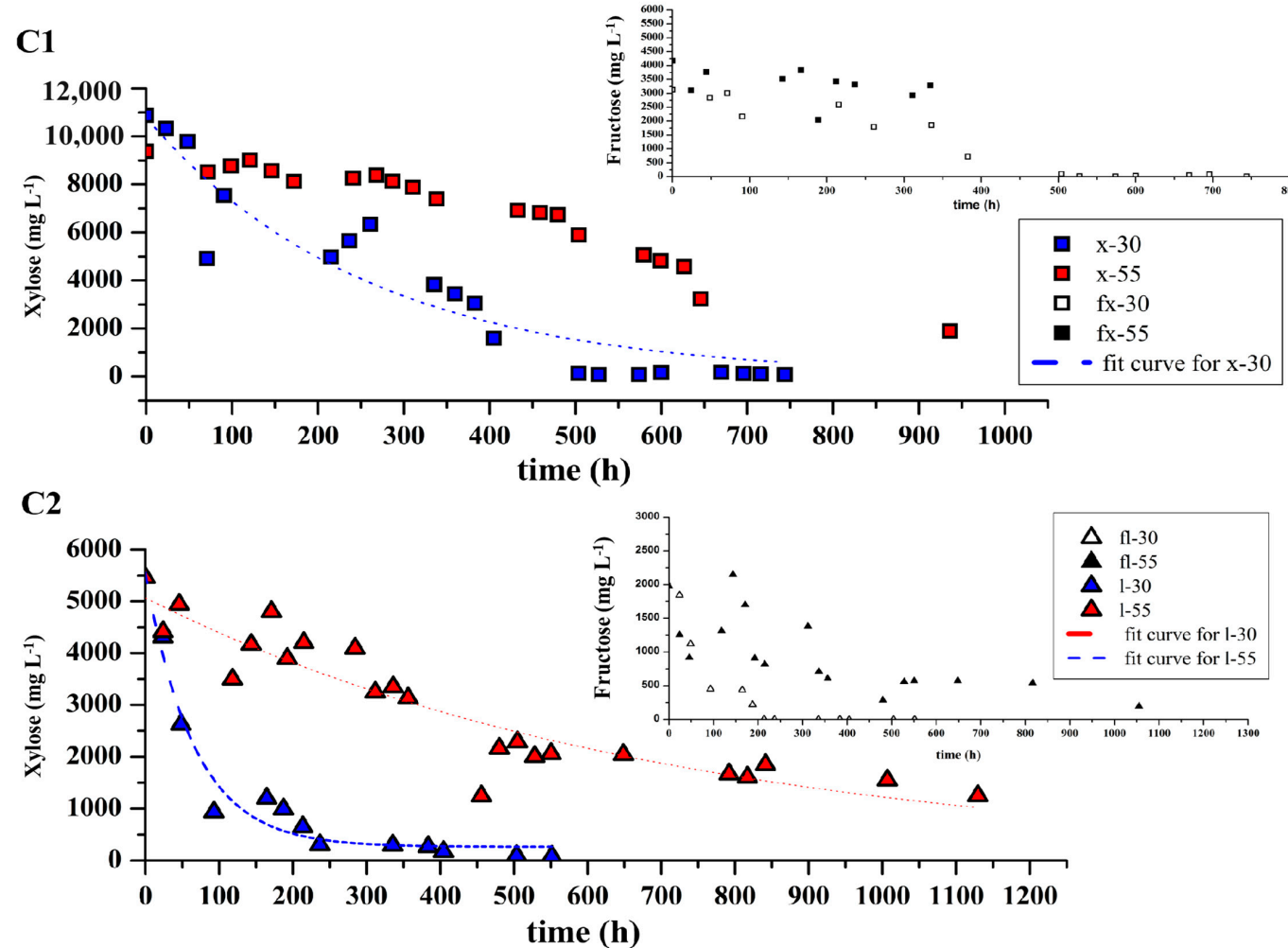


Figure 3. Cont.

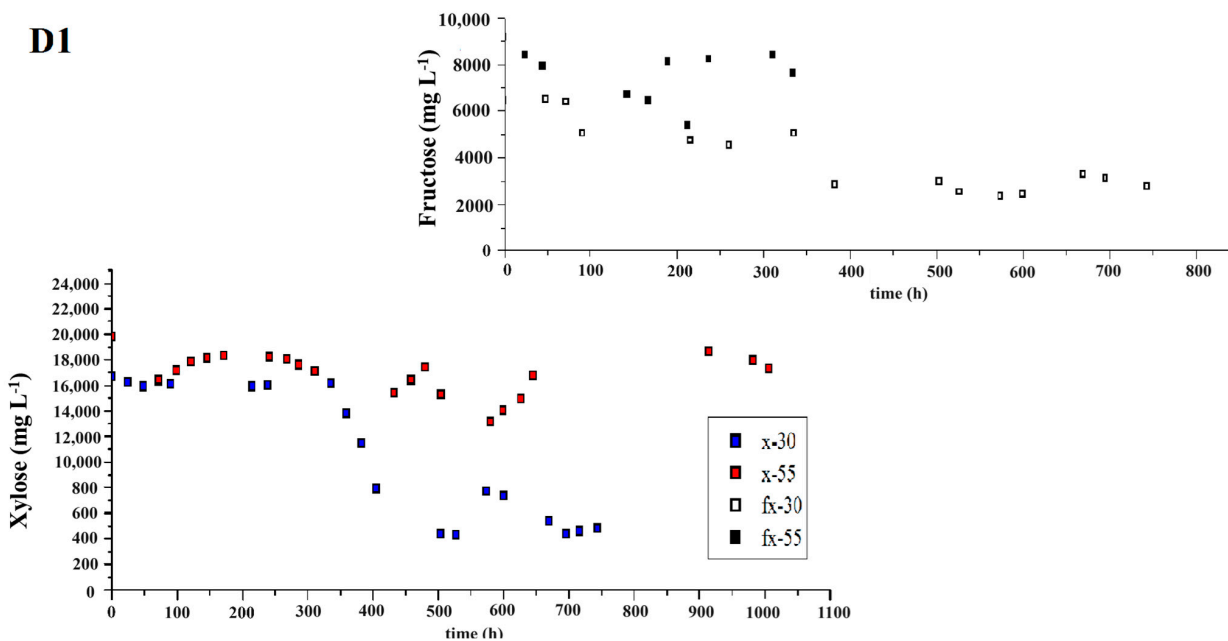
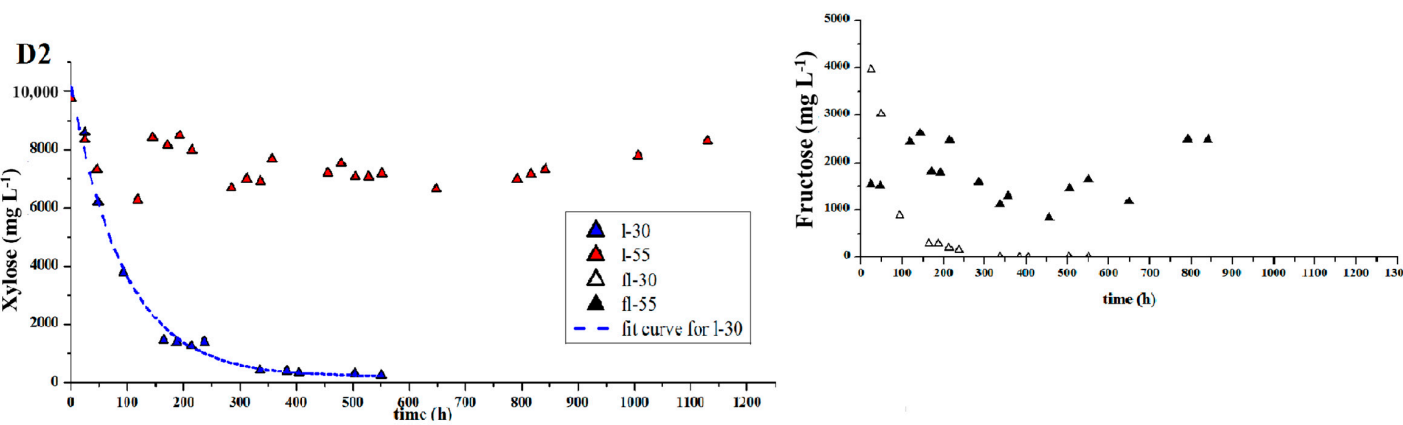
D1**D2**

Figure 3. Cont.

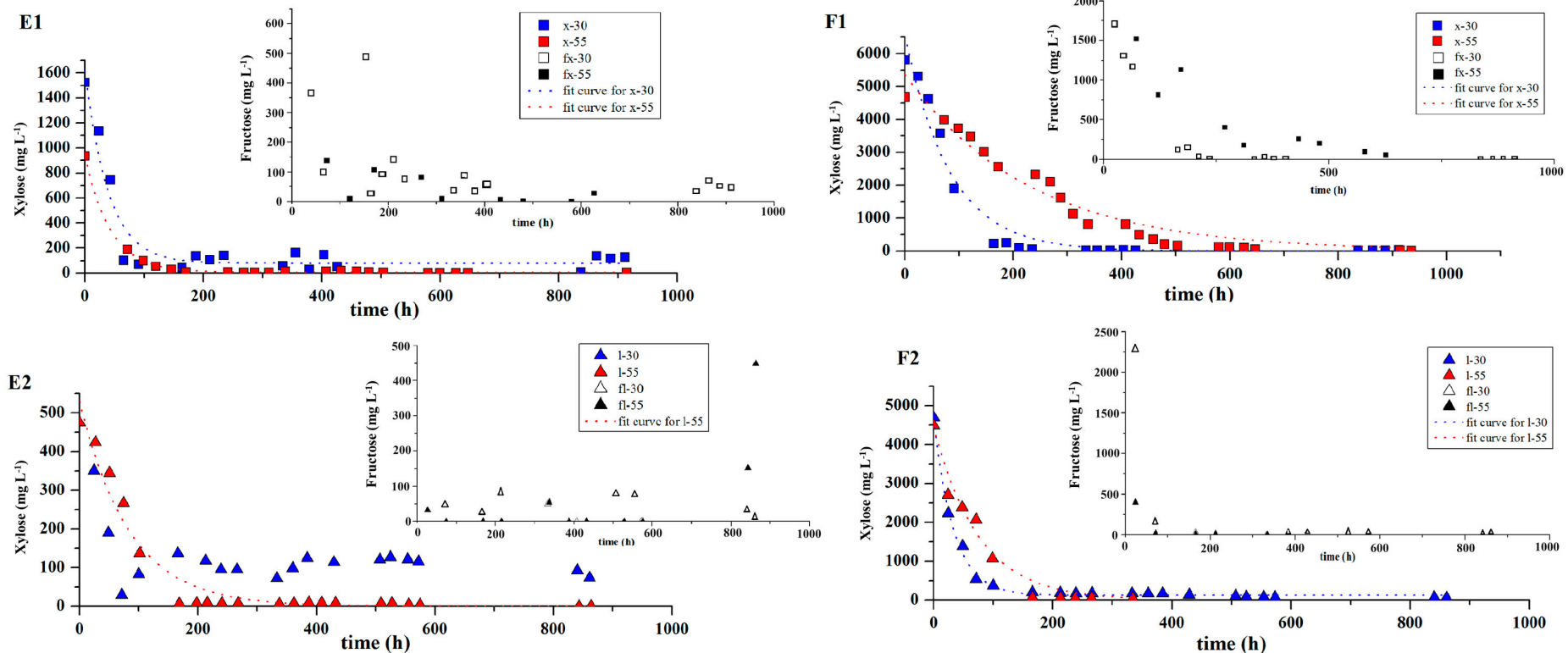


Figure 3. Cont.

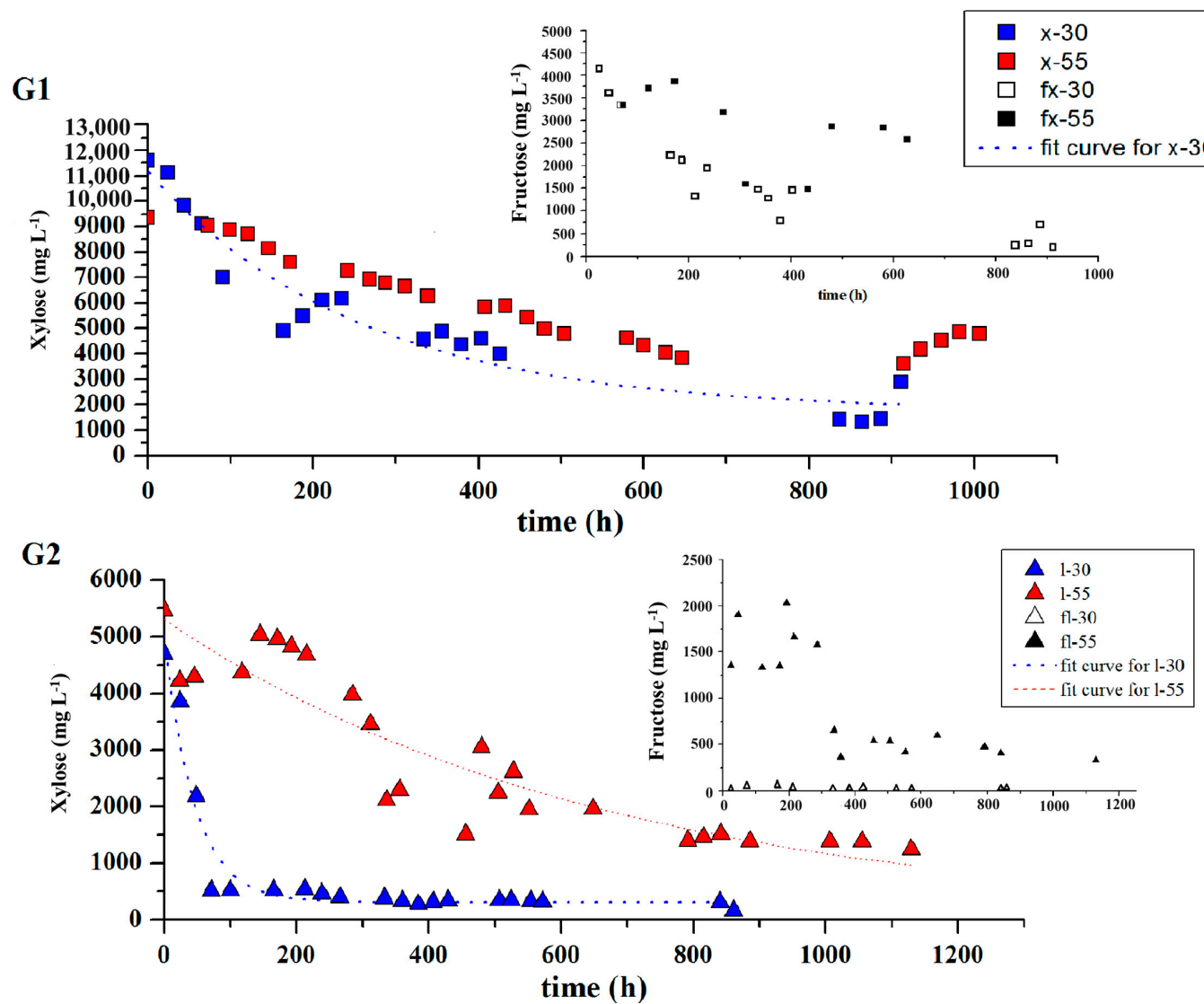


Figure 3. Cont.

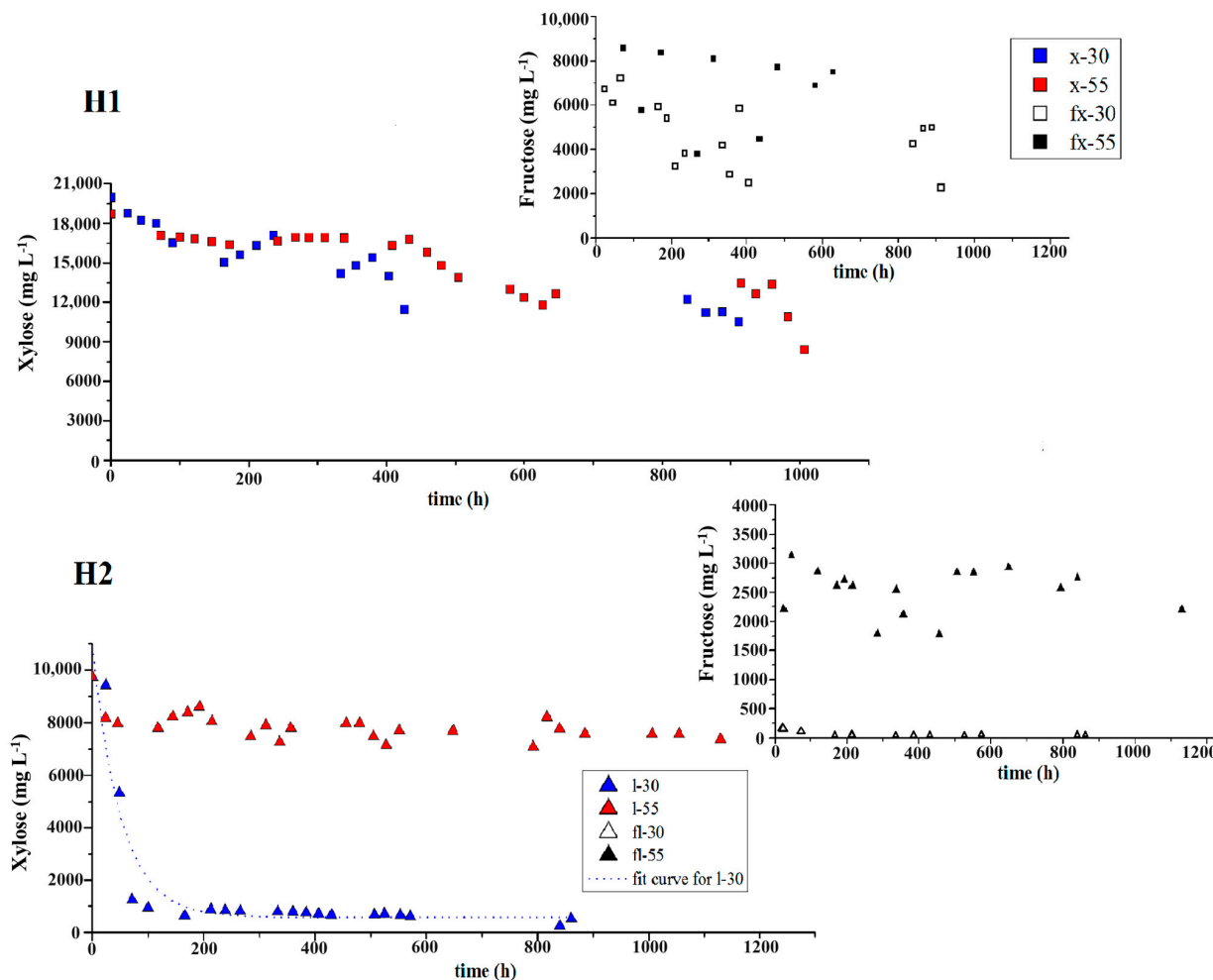


Figure 3. Xylose and fructose degradation at both temperatures (30 and 55 °C). Letters located above each graph indicate specific F/M or C/N ratio: FMI (A1,A2); FMII (B1,B2); FMIII (C1,C2); FMIV (D1,D2); CNI (E1,E2); CNII (F1,F2); CNIII (G1,G2); CNIV (H1,H2). Numbers match reactor types: xylose (1) and pentose liquor (2). Acronyms such as “fx”, “fl”, “x” and “l” correspond to fructose from xylose reactor, fructose from pentose liquor reactor, xylose from xylose reactor and xylose from pentose liquor reactor, respectively. White and blue depict mesophilic temperature (30 °C); black and red represent thermophilic (55 °C) temperature.

Table 2. Soluble metabolic products from all experimental conditions (in terms of mgCOD L⁻¹).

Reactors	Experimental Conditions	Hci (Citric Acid)	Hm (Malic Acid)	Hsu (Succinic Acid)	Hlac (Lactic Acid)	Hf (Formic Acid)	Hac (Acetic Acid)	Hp (Propionic Acid)	Hib (Isobutyric Acid)	Hbu (Butyric Acid)	Hiv (Isovaleric Acid)	Hva (Valeric Acid)	Hca (Caproic Acid)	EtOH (Etha-nol)	MeOH (Methanol)	SMP _{total}
mxr	F/M I	0.89	3.93	8.36	16.21	9.13	49.46	11.34	8.76	29.88	6.69	138.74	0.00	108.01	28.53	419.95
	F/M II	2.10	8.71	23.82	77.62	13.19	109.42	7.21	9.25	180.09	67.90	17.00	0.00	407.28	48.71	1035.30
	F/M III	6.60	11.95	29.42	387.48	34.67	281.37	10.83	22.77	12.36	132.41	53.45	2.85	1067.51	37.47	2091.16
	F/M IV	3.76	18.27	37.54	649.45	35.40	406.85	12.70	13.15	31.20	209.49	86.74	0.00	1691.69	64.47	3260.72
mplr	F/M I	3.88	2.37	14.00	18.25	14.63	280.95	38.37	17.93	219.70	15.40	86.48	124.45	0.00	0.00	835.44
	F/M II	3.33	12.51	33.83	14.08	16.46	673.50	91.72	54.80	435.73	26.20	149.04	357.73	0.00	381.89	2250.83
	F/M III	4.62	8.10	162.92	147.41	22.17	1222.06	148.41	172.98	579.18	45.44	10.28	310.23	0.00	921.00	3754.80
	F/M IV	7.30	11.52	269.02	167.62	21.96	1409.78	497.69	375.37	657.49	137.04	251.39	190.96	0.00	0.00	3997.14
txr	F/M I	2.78	20.62	5.15	185.39	14.14	65.46	6.45	16.61	18.72	20.81	11.76	0.00	3.72	3.67	375.28
	F/M II	11.03	18.00	9.14	186.42	13.19	92.06	9.10	33.00	7.10	19.75	9.53	0.00	22.58	0.67	431.56
	F/M III	4.08	9.04	9.92	57.88	10.91	139.66	7.63	17.36	92.91	14.08	0.00	9.57	23.51	0.00	396.57
	F/M IV	8.80	33.60	11.89	113.41	13.73	120.85	7.29	106.87	18.22	16.30	14.15	16.24	10.45	2.16	493.96
tplr	F/M I	3.10	14.19	15.81	35.06	23.41	250.80	2.86	24.54	202.42	24.40	9.11	5.84	0.00	0.00	611.53
	F/M II	4.11	14.86	100.96	63.64	20.79	625.79	6.25	8.79	323.16	39.26	6.54	26.68	0.00	0.00	1240.81
	F/M III	6.98	18.63	85.84	167.38	28.04	1179.37	16.54	94.73	619.06	87.23	8.82	81.53	0.00	0.00	2394.16
	F/M IV	7.05	27.23	44.52	711.02	40.80	1347.06	22.82	179.79	616.02	47.37	13.11	73.38	0.00	0.00	3130.16
mxr	C/N I	2.36	5.96	5.34	3.28	15.89	241.72	29.76	21.70	160.46	9.99	2.60	5.71	0.00	0.86	505.65
	C/N II	2.35	2.80	12.87	3.39	12.85	468.41	65.00	26.97	881.39	14.69	2.38	21.53	0.00	215.23	1729.87
	C/N III	2.47	5.60	15.95	2.40	16.28	426.46	173.77	80.96	927.56	36.12	8.71	29.90	29.87	1261.75	3017.82
	C/N IV	2.65	11.96	21.92	11.36	14.99	379.48	191.35	63.97	767.95	11.03	6.61	16.10	22.78	2845.25	4367.40
mplr	C/N I	2.77	4.22	14.92	12.98	14.09	328.75	25.82	7.43	13.98	30.79	40.63	14.26	0.00	0.00	510.65
	C/N II	3.13	7.78	27.17	6.79	11.73	871.10	128.48	28.27	107.45	27.08	128.76	33.48	0.00	981.62	2362.86
	C/N III	3.88	6.77	47.30	8.32	10.21	869.92	227.08	24.33	80.49	34.80	35.72	35.04	0.00	430.98	1814.84
	C/N IV	3.33	13.13	126.51	9.02	11.54	1477.81	349.28	98.50	87.28	37.85	46.22	23.25	0.00	1300.96	3584.69

Table 2. Cont.

Reactors	Experimental Conditions	Hci (Citric Acid)	Hm (Malic Acid)	Hsu (Succinic Acid)	Hlac (Lactic Acid)	Hf (Formic Acid)	Hac (Acetic Acid)	Hp (Propionic Acid)	Hib (Isobutyric Acid)	Hbu (Butyric Acid)	Hiv (Isovaleric Acid)	Hva (Valeric Acid)	Hca (Caproic Acid)	EtOH (Etha-nol)	MeOH (Methanol)	SMP _{total}
txr	C/N I	2.32	1.55	5.41	21.42	12.94	217.70	6.70	31.73	145.50	34.67	1.68	13.76	0.00	0.00	502.33
	C/N II	2.78	2.26	7.40	11.45	12.32	506.29	9.29	2.03	296.56	84.93	0.00	24.69	0.00	0.00	960.02
	C/N III	5.92	7.95	5.94	61.48	13.94	476.31	13.75	2.10	386.06	75.59	1.32	11.01	0.00	0.00	1061.38
	C/N IV	3.60	17.97	7.00	180.44	14.35	318.28	20.05	2.27	231.27	42.84	1.17	0.00	0.00	0.00	839.25
tplr	C/N I	2.60	1.60	7.00	6.17	14.33	197.80	8.60	11.41	49.47	27.97	4.84	3.71	0.00	0.00	335.79
	C/N II	2.40	3.65	13.92	9.95	20.06	518.85	8.59	40.05	171.46	34.08	13.86	34.00	0.00	0.00	870.87
	C/N III	11.05	20.59	85.49	159.45	27.26	1076.47	7.12	56.48	567.40	77.61	5.75	45.01	1.97	0.00	2141.60
	C/N IV	17.61	43.47	63.90	977.04	58.12	1865.24	20.31	328.99	147.67	72.59	2.72	0.00	0.00	0.00	3597.64

Table 3. Main ratios of soluble substances and pH values from all experimental conditions.

Reactors	Experimental Conditions	Hbu/SMP _{total}	Hac/SMP _{total}	EtOH/SMP _{total}	Hbu/Hac	Hac/EtOH	pH Initial	pH Final
mxr	F/M I	0.07	0.11	0.26	0.60	0.46	6.4	4.0
	F/M II	0.17	0.10	0.39	1.65	0.27	6.4	3.5
	F/M III	0.006	0.13	0.50	0.04	0.26	6.3	3.0
	F/M IV	0.009	0.12	0.51	0.08	0.24	6.1	2.9
mplr	F/M I	0.26	0.34	0.00	0.78	-	5.3	4.7
	F/M II	0.19	0.30	0.00	0.65	-	6.0	4.2
	F/M III	0.15	0.32	0.00	0.47	-	6.1	4.3
	F/M IV	0.16	0.35	0.00	0.47	-	6.6	5.3
txr	F/M I	0.05	0.17	0.01	0.29	17.66	7.1	3.1
	F/M II	0.02	0.21	0.05	0.08	4.08	6.0	3.6
	F/M III	0.23	0.35	0.06	0.66	5.94	6.1	3.5
	F/M IV	0.04	0.24	0.02	0.15	11.56	6.1	3.6

Table 3. *Cont.*

Reactors	Experimental Conditions	Hbu/SMP _{total}	Hac/SMP _{total}	EtOH/SMP _{total}	Hbu/Hac	Hac/EtOH	pH Initial	pH Final
tplr	F/M I	0.33	0.41	0.00	0.81	-	6.0	4.8
	F/M II	0.26	0.50	0.00	0.51	-	6.9	4.7
	F/M III	0.26	0.49	0.00	0.52	-	6.7	4.6
	F/M IV	0.20	0.43	0.00	0.46	-	6.4	4.6
mxr	C/N I	0.32	0.48	0.00	0.66	-	6.6	4.5
	C/N II	0.51	0.27	0.00	1.88	-	6.0	3.9
	C/N III	0.30	0.14	0.01	2.17	14.3	5.7	3.5
	C/N IV	0.18	0.09	0.005	2.02	16.66	5.3	3.6
mplr	C/N I	0.03	0.64	0.00	0.04	-	6.0	6.4
	C/N II	0.04	0.36	0.00	0.12	-	6.1	4.6
	C/N III	0.04	0.48	0.00	0.09	-	6.1	5.2
	C/N IV	0.02	0.41	0.00	0.06	-	6.1	5.3
txr	C/N I	0.29	0.43	0.00	0.67	-	6.0	4.3
	C/N II	0.30	0.52	0.00	0.59	-	5.8	3.8
	C/N III	0.36	0.45	0.00	0.81	-	6.1	3.6
	C/N IV	0.27	0.38	0.00	0.73	-	6.1	3.5
tplr	C/N I	0.15	0.58	0.00	0.25	-	6.1	5.0
	C/N II	0.19	0.59	0.00	0.33	-	6.0	4.6
	C/N III	0.26	0.50	0.0009	0.53	546.43	6.5	4.6
	C/N IV	0.04	0.52	0.00	0.08	-	6.6	4.7

4. Discussion

4.1. H_2 and SMP Production Outlook Using Thermophilic and Mesophilic Reactors under F/M and C/N Ratios

The sigmoidal curve model adopted in this study did not fit the H_2 curve for mplrs. The instability of the fermentation process (in terms of pH maintenance in certain intervals of values, suitable H_2 pressure, presence of toxic compounds, etc.) probably acted as a preponderant factor for low H_2 production in the abovementioned reactors.

Temperatures in the thermophilic range tend to favor hydrogen production in virtue of lowering H_2 pressure into liquid media by the increase in the gas escape rate from it. In addition, it should be taken into account that the hydrolysis of complex substances is a limiting step in dark fermentation as the organic molecules lie “hidden” inside the microbial cell wall or entangled in an extracellular polymeric matrix, and their breakdown is carried out by extracellular enzymes. Therefore, it is expected that elevated temperatures enhance the dissolution of biodegradable content and also the releasing of hydrolytic enzymes from thermophilic bacteria into aqueous media [45,46].

Although a simple sugar (xylose) as the main substrate was applied to the xrs, the sludge used as seed for the fermentation process itself contained a bulk of organic substances entrapped in cell walls or extracellular matrices which did not allow efficient contact between the microorganisms and the biodegradable content (xylose and fructose). Diverse comparative studies using either complex (cellulose and starch, for instance) or simple sugars reported higher H_2 production at thermophilic temperatures than mesophilic ones [10–12,47].

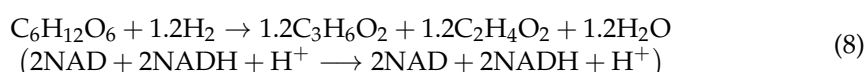
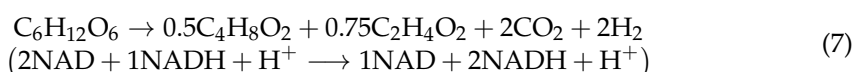
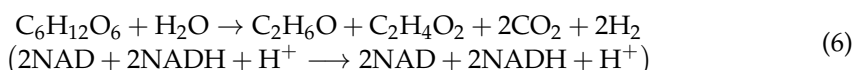
In the thermophilic range, H_2 -consuming bacteria have limited growth. Regarding bacterial diversity inside sewage seed, it is more probable we will find, proportionally, a larger number of thermophilic H_2 -producing bacteria species than mesophilic H_2 -producing strains [48,49].

When evaluating the influence of different temperatures on H_2 production from anaerobic mixed flora using batch reactors and xylose as the main substrate, the authors in [19] found higher HPRs in the mesophilic range (30–40 °C) than thermophilic conditions (45–55 °C). It is not necessarily mandatory that the highest values of HPR and HY are found at the same experimental temperature. High HPRs tend to be reached in mesophilic conditions due to the presence of low cell densities in outward flow, while high HYS in thermophilic conditions are related to slow growth rates observed in extremophilic microorganisms [50]. Ref. [10] performed a comparative study adopting mesophilic and thermophilic temperatures to H_2 production. They used a preheated mesophilic anaerobic digester sludge as inoculum and reported, using starch as substrate, a maximum hydrogen production rate (MHPR) of 5 at 60 °C and 11 mL h⁻¹ at 37 °C while HYS were 1.13 (60 °C) and 1.00 mol H_2 mol hexose_{added}⁻¹ (37 °C). The initial mesophilic characteristic of anaerobic seed adopted in the present study, as in [10], might have affected kinetic parameters related to the H_2 production rate in the thermophilic range. However, as these cells have low proliferation rates, they showed, at least in most of the tpls, higher HYS in comparison to mplrs.

It is worth mentioning that there is no consensus about which temperature range is better for hydrogen production through dark fermentation. Previous work [51], for example, reported higher HY at mesophilic temperature (37 °C) than thermophilic (55 °C): 1.8 and 1.0 mol H_2 mol glucose⁻¹, respectively. On the other hand, [11] found higher cumulative hydrogen production (171 mL), HY (111 mL H_2 g total sugar⁻¹), and SHPR (3.46 mL H_2 L⁻¹ h⁻¹) at 55 °C when compared to 37 °C using cheese whey powder solution as substrate. In addition to the mesophilic or thermophilic H_2 production being related to seed enrichment with H_2 producers, other factors should be considered, such as the inoculum type, the substrate adopted as the carbon source, the hydraulic reactor regime, and the mineral supplements applied.

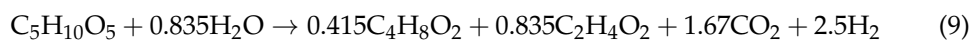
Evaluation of nutritional requirements such as F/M or C/N ratios have been presented in previous studies [52–55] as important operational parameters to achieve better H₂ production rates in distinct types of substrates used during the dark fermentation process. Ref. [51] evaluated the influence of the C/N ratio in an H₂ production context using palm oil effluent. The authors observed optimum hydrogen generation at C/N = 140 and a reduction of this gas at C/N = 190, showing that the nitrogen deficiency could affect microorganism metabolism, such as those related to H₂ production. Apart from this, taking the F/M ratio into consideration, ref. [52] reported over a F/M range of 1.5–38.2 (as in the present study) with a prominent HY value of 137.73 mLH₂.g substrate⁻¹ at F/M = 38.2 using condensed molasses as substrate in a batch reactor. There is a wide variation in values of organic load ratios, which enhance quantities of cumulative H₂ produced, or even improve values of HYs. Likewise, regarding the influence of temperature, varying numbers regarding feed ratios seem to lie in the uniqueness of microbial seeds, chosen substrate, working temperature, initial organic load level applied, and hydraulic regime.

The proportion of SMPs such as acetate, butyrate, propionate, and ethanol in liquid bulk contributes to evaluating the fermentation stability and the HY itself. Concerning ethanol, the known ethanol-type fermentation is associated with several fermentative reactions that globally result in ethanol production accounting for almost 30% (calculated as equivalent COD) of total SMPs, and the quantity of acetate and ethanol together is more than 50% of the total produced by fermentation in liquid bulk [44]. Anaerobic process stability often focuses on evaluating VFA (acetate, butyrate, and propionate) concentrations, although some authors have associated better H₂ production and overall process stability by analyzing ethanol-type fermentation [18,56,57]. The balance between NAD⁺/NADH + H⁺ of approximately 1:1 is essential to ensure a suitable intracellular pH and continuous hydrogen production. For ethanol or propionic acid generation, as well as acetate, 2 moles of NADH + H⁺ are formed through glucose degradation to produce 2 moles of pyruvate, one of which generates 1 mol of acetate (without NAD⁺ formation), and the other generates 1 mol of ethanol/propionate which produces 2 moles of NAD⁺; thus, a dynamic equilibrium between reduced and oxidized forms of the nicotinamide molecule [56,58] is achieved. Therefore, the closer the ethanol/acetate ratio to one, the more stable the fermentative metabolism and biohydrogen production will be [59]. The probable ethanol-type occurrence under mxr-FMII, mxr-FMIII, and mxr-FMIV conditions showed the closest values of optimum ethanol/acetate ratio (except for mxr-FMI): 0.27 (mxr-FMII), 0.26 (mxr-FMIII) and 0.24 (mxr-FMIV) (Table 3). The propionic pathway (Equation (8)), however, consumes H₂ and produces acidic forms that contribute to reducing pH, hindering the fermentation process. Comparing ethanol-type fermentation to butyrate-type (Equations (6) and (7), respectively), the first provides more fermentation stability, whilst the second yields the same 2 H₂ moles per hexose but produces a theoretical NAD⁺/NADH + H⁺ ratio of 1:2, leaving the fermentation process unstable [57].

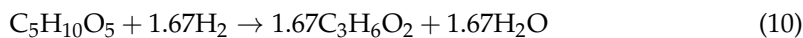


Considering the availability of NADH + H⁺ as a precursor to H₂ formation through ferrodoxin reduction, butyrate-type fermentation has a higher potential to produce H₂ than ethanol-type fermentation, in virtue of higher NAD_{reduced} concentration. However, the stability of the anaerobic process is hindered (H₂ production as well) eventually due to an imbalance between NAD⁺/NADH + H⁺ forms, resulting in acidification of bulk media. Some authors consider that the HBu/HAc ratio is proportional to HYs [47,60],

and some of them suggest that the ideal ratios to find the highest HYs are 1.6–2.2 [60–62]. Other authors reported greater results in HY with the HBu/HAc ratio above 2.6 [63–65]. Theorizing acetate and butyrate production by xylose degradation, this metabolic pathway would be able to yield $2.5 \text{ mol H}_2 \text{ mol xylose}^{-1}$ and an HBu/HAc ratio of 0.5 (Equation (9)). None of the batches reached this HY value (or close to it) as a result of limiting factors, which is further discussed. The HBu/HAc ratio analyses only make sense for butyrate-type fermentation that appears when butyrate encompasses 30% of the total SMPs and the sum of butyrate and acetate exceeds 50% of fermentation products [44]. In the present study, the butyrate-type fermentation has possibly been found in tplr-FMI, mxr-CNI, mxr-CNII, mxr-CNIII, txr-CNII, and txr-CNIII conditions (Table 3). The low Hbu/SMP_{total} values in most of the plrs could be explained by a high initial concentration of acetate in comparison to other VFAs, such as butyric acid. A higher relative presence of butyrate at thermophilic rather than mesophilic reactors might be related to lower VFA production at elevated temperatures. Thermophilic conditions tend to produce H₂ from traditional acetate or butyric routes in a stable way, often without a considerable amount of other VFA compounds.



Propionic acid is one of the VFAs that must be constantly monitored over the fermentation period to ensure steady H₂ production. High propionate concentrations in a liquid bulk promote an intense cellular pH drop, collapsing the fermentative process. Through xylose degradation, 1.67 moles of H₂ are consumed per mole of C5 sugar, yielding 1.67 moles of propionate per mol of substrate (Equation (10)). The propionic acid-type fermentation can be determined as the propionate reaches between 15–20% of the total SMPs [44]. The mplr-FMIV condition possibly showed propionic acid-type fermentation due to high propionate production allied to its low HY.



Some studies reported acetate and lactate as the main intermediate SMPs at 70 °C using sucrose [66] and xylose [67] as main substrates. Lactic producers are commonly found at mesophilic temperatures competing with other fermentative bacteria and many of them are not able to degrade xylose-rich compounds [68]. Previous works reported the existence of one solely thermophilic lactate producer named *Bacillus coagulans* [69,70] which can degrade both glucose and xylose sugars under 50–55 °C using simpler culture media such as MRS medium [71]. As lactic acid produced through several conditions in the present study was accomplished with considerable production of acetate, formate, and in some cases, butyrate (Figure 2 and Table 2), it is reasonable to assume lactate formation through the heterofermentative pathway derived from previous xylose breakdown by the phosphoketolase pathway (discussed in detail later). Basically, two alternative metabolic routes simultaneously appear: (1) The breaking of xilulose-5P into glyceraldehyde 3-P (GAP), followed by pyruvate generation, and lastly lactate or formate; and (2) production of acetil-P through the phosphoketolase pathway by the presence of xilulose-5P, followed by acetate production or acetil-CoA generation from acetil-P, and further formation of acetate, butyrate, ethanol, etc. [62,72].

Isobutyrate can be produced by thermophilic bacteria which are able to transform pyruvate molecules from glycolysis into isobutyraldehyde (in a similar way to the Ehrlich pathway in amino acid degradation) using the 2-ketoacid decarboxylase enzyme [73]. It is probable that greater carbon availability under FMIV conditions have contributed to larger metabolic route diversification.

Medium-chain fatty acids (MCFAs) are the result of carbon chain elongation from short-chain fatty acids (SCFAs) such as acetic, butyric, and lactic acids without necessarily being coupled with hydrogen production. Higher SCFA concentrations in mplr-FMs (Table 2) might have allowed further carbon chain elongation in possible metabolic pathways. In a

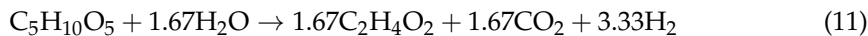
previous study [74], among the diverse routes of caproate production cited, the authors suggested the formation of this acid along with H₂ by anterior ethanol dehydrogenation. As there was no ethanol presence in mplr-FMII, it is more reasonable to assume caproate production from acetate and/or butyrate with H₂ as the electron donor.

As methanol was reported in plrs, its presence could be explained by dissociation of methyl and methoxy groups from lignin and hemicellulose polymers during acid pre-treatment of sugarcane bagasse at elevated temperatures [75]. How would the existence of methanol be explained in xrs and its increasing production throughout the fermentation process? The methanol found in mxr-CNII, mxr-CNIII, and mxr-CNIV must have originated from poultry slaughterhouse inoculum. The use of glycerin from the biodiesel industry as a food complement in poultry diets is common in Brazil [76]. During the industrial biodiesel process, excess methanol is reacted with glycerin, and a considerable quantity of this alcohol is not separated after the end of the reaction. Continuous production in some conditions (mplr-CNII, mplr-FMIII, and mplr-CNIV, for example) suggests the metabolic production of methanol from microorganisms with enzymes such as pectin methylesterase (acts on methoxyl esters), found in some *Clostridium* strains [77]. To date, there is no description of any presence of methanol in metabolic reactions associated with H₂.

In general, at hot temperatures, few microorganisms are capable of surviving, and thus, a poor variety of metabolic routes is observed with predominance of some thermophilic strains of *Clostridium*. Fewer SMPs generated during the fermentation process at 55 °C indicate less availability of carbon sources, and consequently a reduced number of metabolic pathways related to H₂ when compared to mesophilic temperatures.

4.2. H₂ Production Drawbacks from Non-Fermentative Products

Considering the maximum HY of 3.33 mol H₂ mol xylose⁻¹ when acetate is a byproduct (Equation (11)) and the values of HYs observed in the present study, there was no similar yield registered under any experimental conditions. Aside from the H₂ production by aforementioned fermentation types which yielded low HYs, this section intends to bring other issues faced in obtaining high HYs to light.



Certain aspects of substrate degradation might be related to lower HYs than those theoretically expected. Glucose and fructose are commonly preferentially metabolized by the most anaerobic microorganisms once the glycolytic pathway is present in all known fermentative bacteria in opposition to efficient xylose-degrading enzymatic machinery. Evidence that glucose transporters found in *Saccharomyces cerevisiae* can also accomplish xylose uptake but at the cost of much lower rates [78] might also be assumed to exist in fermentative bacteria; this is quite probable. As no bioaugmentation with xylose-degrading strains took place, it is reasonable to assume low xylose uptake rates. Depending on the origin of the mixed culture adopted, higher HYs can be obtained in reactors fed with xylose rather than glucose as shown by [79].

D-xylose is not readily degraded as glucose and fructose, because this C5 sugar does not go directly to the glycolysis pathway. Instead, it is converted into D-xylulose-5-phosphate (X5P). This metabolite can follow two separate ways: the pentose phosphate pathway (PPP), or the phosphoketolase pathway (PKP) [80]. The PPP consists of a set of X5P rearrangement reactions into different sugars to generate glyceraldehyde-3-phosphate (G3P), one of the most important intermediates of glucose metabolism [79]. In the PKP, X5P is cleaved into G3P and acetylphosphate. The latter is converted into acetate [71]. Preferential acetate production by PKP leads to a lesser possibility of H₂ formation as only 1 mole of G3P is generated per mole of xylose, while the PPP produces 2 G3P molecules per mole of xylose.

Substrate inhibition was not an issue we could overlook, as xylose concentrations were increasing during the experimental plan. Several authors reported substrate inhibition in xylose-rich media at different concentrations with different seeds: 10 g L⁻¹ using mixed

culture [81], 15 g L⁻¹ with isolated strain [82], and 20 g L⁻¹ with pure culture [83]. This substrate concentration range was adopted in the present study. The substrate inhibitions should have occurred as of 10 g L⁻¹ in trs and at 20 g L⁻¹ in mxrs. It is worth remembering that xylose concentrations measured in plrs were lower than in xrs due to the presence of other substances in the hydrolysate which accounted for the increase in COD measurements. High initial acetate concentrations exhibited in plrs (Table S1) should be taken into consideration to evaluate ongoing xylose degradation in these reactors.

The mesophilic feature of microflora showing a substantial number of xylose-degrading species in mild conditions when compared to thermophilic seeds may explain lower k_1^{app} values therein. It is worth noting that high k_1^{app} values do not necessarily mean higher H₂ yields. To illustrate this [10], using mesophilic seeds reported higher HYs both at thermophilic cellulose-only and starch-only batches compared with mesophilic ones, although the overall specific utilization rate (r_{su}/X) values were higher in mesophilic conditions. Instead of hydrogen, higher k_1^{app} values seem to head the production of SMP byproducts. Elevated temperature conditions that had lower k_1^{app} numbers and high H₂ yields were supported by low cell quantities, associated with a small proportion of H₂-consumers concomitant with an elevated percentage of H₂-producers. As discussed in the previous section and through all the content in this paragraph, the occurrence of higher HPRs in mxrs than txrs, and greater HYs in the latter under a pairwise comparison context is not surprising (Table 1).

H₂ inhibitory compounds such as acetate, furfural, hydroxymethylfurfural (HMF), and phenolic derivatives are produced with acid pretreatment hydrolysis of sugarcane bagasse. Excess of acetic acid can lead to a reduction in intracellular pH causing fermentation inhibition [84]. Moreover, furan substances may affect the glycolysis enzymes and cause DNA damage in some fermentative bacteria [85]. Meanwhile, phenolic compounds may alter the cell membrane permeability, hindering the fermentation process [86].

Based on several studies [85,87–89], furan derivatives and phenolic compounds show an inhibitory effect on H₂ production in concentrations of up to approximately 1 g L⁻¹. These toxic compounds commonly worsen hydrogen generation in concentrations close to 1 g L⁻¹, which is quite improbable to have been found in any plr. Values of furfural were reported close to 1 g L⁻¹ by [90] when dilute acid pretreatment of sugarcane bagasse (2% H₂SO₄ (v/v), 122 °C, and 60 min) was used. A previous study [86], promoting corn stover hydrolysis (2% H₂SO₄ (v/v), 121 °C, and 90 min), obtained 0.1 g L⁻¹ of phenolic compounds and 0.85 g L⁻¹ of furan derivatives. These works applied higher temperatures and acid concentration in the hydrolysis process of sugarcane bagasse compared to the present study. Furthermore, proper xylose and COD concentrations were achieved after further dilution of hydrolysate.

There is no consensus regarding the threshold acetate concentration for H₂ inhibition, but it seems to be found at high concentrations (up to 5 g L⁻¹), with which some related issues were noticed [91–94]. In [90], the authors applied a mixed seed with glucose as a carbon source exhibiting an inhibition constant (K_c) of 8.27 g L⁻¹ of acetate for H₂ production. Using mixed seed and glucose as feed, Ref. [91] showed a decrease of 50% at HPR (mL h⁻¹) when 6 g L⁻¹ of acetate was added. Considering that the highest acetic acid concentration found in plrs was lower than 2.5 g L⁻¹ (mplr-FMIV) (Table S1), its inhibitory effect on H₂ production seems unexpected and hard to measure in the present study.

High sulfate concentrations were found at higher xylose concentrations in plrs due to sulfuric acid dissolution in the hydrolysis process (Table S1). Sulfate in high concentrations leads to a reduction in H₂ production by the proliferation of sulfate-reducing bacteria (SRB). Some SRBs can lead to sulfate reduction using H₂ as an electron donor and non-complex molecules such as acetate or ethanol as carbon sources [95]. However, this metabolic pathway hardly took place in plrs, as SRB are not able to survive at low pH values (<5.5) commonly presented in fermentative processes [96].

5. Conclusions

Sugarcane bagasse pentose liquor is a feasible source of fermentative hydrogen. This highly pollutant agro-waste becomes an economic asset, being a raw material for energy carrier production, and at the same time, having a clean destination for it, avoiding the pollution of streams. In general, hydrolysate reactors under thermophilic temperatures showed higher HYs and cumulative hydrogen production than mesophilic ones. Elevated temperatures can ensure better contact between substrate and microorganisms, inhibit most H₂ consumers, and enable favorable thermodynamic conditions for hydrogen release from liquid bulk media.

Variations in F/M and C/N ratios mostly implied significant HY differences even at the same temperature. Relevant discrepancies were also verified under both mesophilic and thermophilic environments for the same F/M or C/N ratio. Therefore, nutritional and temperature aspects might have affected the hydrogen production parameters.

Diversification of experimental conditions drove H₂ production through several fermentation types (ethanol, butyric, and propionic-fermentation types), where acetate was one of the main SMPs in a large majority of reactors. Other SMPs also had prominent production in at least one condition. The unusual detection of methanol in substantial quantities under some experimental conditions appeared to be intricately connected with it being embedded into the inoculum. It could also have been produced by microorganisms from sludge which contained enzymes, such as pectin methylesterases.

Aside from bacteria competition and their fermentative products, important drawbacks for H₂ production seemed to be more related to constraints concerning xylose uptake. Occurrences of substrate inhibition at high xylose concentrations fitted better as a response to poor H₂ production than toxic substances such as acetate, furan derivatives, and phenolic compounds presented therein.

Supplementary Materials: The following supporting information can be downloaded at: <https://www.mdpi.com/article/10.3390/fermentation10080432/s1>, Table S1: Soluble substances under initial experimental conditions.

Author Contributions: L.M.-F. performed all laboratory activities and promoted initial data organization through writing some initial ideas and designing graph concepts. G.M. assisted L.M.-F. with laboratory activities and answered her questions, put together the experimental design of this research, and contributed with a discussion and data analysis while carrying out the experiment. G.P. contributed to laboratory tasks, helped in the discussion and data analysis during and after the experiment. F.V.F. wrote the present manuscript, created the final graphs and figures, and performed the data discussion according to the focus given to the present text. M.Z. coordinated the task group, contributed with ideas, suggestions, and analyses during the experimental part, and helped with the discussion section written in the present manuscript. All authors have read and agreed to the published version of the manuscript.

Funding: Most authors had scholarships provided by Fundação de Amparo à Pesquisa do Estado de São Paulo (FAPESP—Process number 2009/15984-0) or Conselho Nacional de Desenvolvimento Científico e Tecnológico, Brazil (CNPq—Process number 304540/2021-8). These governmental financial agencies along with another called Coordenação de Aperfeiçoamento de Pessoal de Nível Superior (CAPES) also financially supported this research by helping to buy necessary equipment and materials and to pay for technical maintenance of some laboratory apparatus.

Institutional Review Board Statement: Not applicable.

Informal Consent Statement: Not applicable.

Data Availability Statement: The original contributions presented in the study are included in the article/supplementary material and further inquiries can be directed to the corresponding author.

Acknowledgments: The authors are thankful for the financial support from the following governmental agencies: Fundação de Amparo à Pesquisa do Estado de São Paulo, Conselho Nacional de Desenvolvimento Científico e Tecnológico, Brazil (CNPq), and Coordenação de Aperfeiçoamento de Pessoal de Nível Superior (CAPES).

Conflicts of Interest: The authors declare no conflicts of interest.

References

1. Eker, S.; Sarp, M. Hydrogen gas production from waste paper by dark fermentation: Effects of initial substrate and biomass concentrations. *Int. J. Hydrogen Energy* **2017**, *42*, 2562–2568. [\[CrossRef\]](#)
2. Arimi, M.M.; Knodel, J.; Kiprop, A.; Namango, S.S.; Zhang, Y.; Geißen, S.-U. Strategies for improvement of biohydrogen production from organic-rich wastewater: A review. *Biomass Bioenergy* **2015**, *75*, 101–118. [\[CrossRef\]](#)
3. Bharathiraja, B.; Sudharsanaa, T.; Bharghavi, A.; Jayamuthunagai, J.; Praveenkumar, R. Biohydrogen and Biogas—An overview on feedstocks and enhancement process. *Fuel* **2016**, *185*, 810–828. [\[CrossRef\]](#)
4. Ghimire, A.; Sposito, F.; Frunzo, L.; Trably, E.; Escudé, R.; Pirozzi, F.; Lens, P.N.; Esposito, G. Effects of operational parameters on dark fermentative hydrogen production from biodegradable complex waste biomass. *Waste Manag.* **2016**, *50*, 55–64. [\[CrossRef\]](#) [\[PubMed\]](#)
5. Phowan, P.; Danvirutai, P. Hydrogen production from cassava pulp hydrolysate by mixed seed cultures: Effects of initial pH, substrate and biomass concentrations. *Biomass Bioenergy* **2014**, *64*, 1–10. [\[CrossRef\]](#)
6. Yasin, N.H.M.; Mumtaz, T.; Hassan, M.A.; Abd Rahman, N. Food waste and food processing waste for biohydrogen production: A review. *J. Environ. Manag.* **2013**, *130*, 375–385. [\[CrossRef\]](#) [\[PubMed\]](#)
7. Lee, D.-Y.; Xu, K.-Q.; Kobayashi, T.; Li, Y.-Y.; Inamori, Y. Effect of organic loading rate on continuous hydrogen production from food waste in submerged anaerobic membrane bioreactor. *Int. J. Hydrogen Energy* **2014**, *39*, 16863–16871. [\[CrossRef\]](#)
8. Khamtib, S.; Reungsang, A. Biohydrogen production from xylose by *Thermoanaerobacterium thermosaccharolyticum* KKU19 isolated from hot spring sediment. *Int. J. Hydrogen Energy* **2012**, *37*, 12219–12228. [\[CrossRef\]](#)
9. Mamimin, C.; Chaikitkaew, S.; Niyasom, C.; Kongjan, P.; Sompong, O. Effect of Operating Parameters on Process Stability of Continuous Biohydrogen Production from Palm Oil Mill Effluent under Thermophilic Condition. *Energy Procedia* **2015**, *79*, 815–821. [\[CrossRef\]](#)
10. Gupta, M.; Gomez-Flores, M.; Nasr, N.; Elbeshbishi, E.; Hafez, H.; El Naggar, M.H.; Nakhla, G. Performance of mesophilic biohydrogen-producing cultures at thermophilic conditions. *Bioresour. Technol.* **2015**, *192*, 741–747. [\[CrossRef\]](#)
11. Kargi, F.; Eren, N.S.; Ozmihi, S. Bio-hydrogen production from cheese whey powder (CWP) solution: Comparison of thermophilic and mesophilic dark fermentations. *Int. J. Hydrogen Energy* **2012**, *37*, 8338–8342. [\[CrossRef\]](#)
12. Cakir, A.; Ozmihi, S.; Kargi, F. Comparison of bio-hydrogen production from hydrolyzed wheat starch by mesophilic and thermophilic dark fermentation. *Int. J. Hydrogen Energy* **2010**, *35*, 13214–13218. [\[CrossRef\]](#)
13. Peintner, C.; Zeidan, A.A.; Schnitzhofer, W. Bioreactor systems for thermophilic fermentative hydrogen production: Evaluation and comparison of appropriate systems. *J. Clean. Prod.* **2010**, *18*, S15–S22. [\[CrossRef\]](#)
14. van Groenestijn, J.W.; Hazewinkel, J.H.O.; Nienoord, M.; Bussmann, P.J.T. Energy aspects of biological hydrogen production in high rate bioreactors operated in the thermophilic temperature range. *Int. J. Hydrogen Energy* **2002**, *27*, 1141–1147. [\[CrossRef\]](#)
15. Kundu, K.; Sharma, S.; Sreekrishnan, T.R. Effect of operating temperatures on the microbial community profiles in a high cell density hybrid anaerobic bioreactor. *Bioresour. Technol.* **2012**, *118*, 502–511. [\[CrossRef\]](#) [\[PubMed\]](#)
16. Pan, J.; Zhang, R.; El-Mashad, H.M.; Sun, H.; Ying, Y. Effect of food to microorganism ratio on biohydrogen production from food waste via anaerobic fermentation. *Int. J. Hydrogen Energy* **2008**, *33*, 6968–6975. [\[CrossRef\]](#)
17. Lucas, S.D.M.; Peixoto, G.; Mockaitis, G.; Zaiat, M.; Gomes, S.D. Energy recovery from agro-industrial wastewaters through biohydrogen production: Kinetic evaluation and technological feasibility. *Renew. Energy* **2015**, *75*, 496–504. [\[CrossRef\]](#)
18. del Pilar Anzola-Rojas, M.; Gonçalves da Fonseca, S.; Canedo da Silva, C.; Maia de Oliveira, V.; Zaiat, M. The use of the carbon/nitrogen ratio and specific organic loading rate as tools for improving biohydrogen production in fixed-bed reactors. *Biotechnol. Rep.* **2015**, *5*, 46–54. [\[CrossRef\]](#) [\[PubMed\]](#)
19. Lin, C.Y.; Lay, C.H. Carbon/nitrogen-ratio effect on fermentative hydrogen production by mixed microflora. *Int. J. Hydrogen Energy* **2004**, *29*, 41–45. [\[CrossRef\]](#)
20. Sreethawong, T.; Chatsiriwatana, S.; Rangsuvigit, P.; Chavadej, S. Hydrogen production from cassava wastewater using an anaerobic sequencing batch reactor: Effects of operational parameters, COD:N ratio, and organic acid composition. *Int. J. Hydrogen Energy* **2010**, *35*, 4092–4102. [\[CrossRef\]](#)
21. Scarlat, N.; Martinov, M.; Dallemand, J.-F. Assessment of the availability of agricultural crop residues in the European Union: Potential and limitations for bioenergy use. *Waste Manag.* **2010**, *30*, 1889–1897. [\[CrossRef\]](#)
22. Fan, Y.-T.; Zhang, Y.-H.; Zhang, S.-F.; Wei, H.; Ren, B. Efficient conversion of wheat straw waste into biohydrogen gas by cow dung compost. *Bioresour. Technol.* **2006**, *97*, 500–505. [\[CrossRef\]](#) [\[PubMed\]](#)
23. Bentsen, N.S.; Felby, C.; Thorsen, B.J. Agricultural residue production and potentials for energy and materials services. *Prog. Energy Combust. Sci.* **2014**, *40*, 59–73. [\[CrossRef\]](#)
24. Rabelo, S.C.; Carrere, H.; Maciel Filho, R.; Costa, A.C. Production of bioethanol, methane and heat from sugarcane bagasse in a biorefinery concept. *Bioresour. Technol.* **2011**, *102*, 7887–7895. [\[CrossRef\]](#)
25. Cardona, C.A.; Quintero, J.A.; Paz, I.C. Production of bioethanol from sugarcane bagasse: Status and perspectives. *Bioresour. Technol.* **2010**, *101*, 4754–4766. [\[CrossRef\]](#) [\[PubMed\]](#)
26. Ferreira-Leitão, V.; Gottschalk, L.M.F.; Ferrara, M.A.; Nepomuceno, A.L.; Molinari, H.B.C.; Bon, E.P.S. Biomass Residues in Brazil: Availability and Potential Uses. *Waste Biomass Valorization* **2010**, *1*, 65–76. [\[CrossRef\]](#)

27. Mariano, A.P.; Dias, M.O.S.; Junqueira, T.L.; Cunha, M.P.; Bonomi, A.; Filho, R.M. Utilization of pentoses from sugarcane biomass: Techno-economics of biogas vs. butanol production. *Bioresour. Technol.* **2013**, *142*, 390–399. [\[CrossRef\]](#)

28. Zhang, L.; Huang, H.; He, T.; Sun, J.; Chen, K.; Yue, F. Highly selective extraction of lignin and hemicellulose with retained original structure from sugarcane bagasse via low-temperature soaking and acidic precipitation. *Ind. Crops Prod.* **2024**, *209*, 118015. [\[CrossRef\]](#)

29. Rabelo, C.A.B.S.; Soares, L.A.; Sakamoto, I.K.; Silva, E.L.; Varesche, M.B.A. Optimization of hydrogen and organic acids productions with autochthonous and allochthonous bacteria from sugarcane bagasse in batch reactors. *J. Environ. Manag.* **2018**, *223*, 952–963. [\[CrossRef\]](#)

30. Cheng, J.; Zhu, M. A novel anaerobic co-culture system for bio-hydrogen production from sugarcane bagasse. *Bioresour. Technol.* **2013**, *144*, 623–631. [\[CrossRef\]](#)

31. Rashidi, M.; Alavi, N.; Amereh, F.; Rafiee, M.; Amanidaz, N.; Partovi, K.; Mosanefi, S.; Bakhshoodeh, R. Biohydrogen production from co-digestion of sugarcane vinasse and bagasse using anaerobic dark fermentation. *Bioresour. Technol. Rep.* **2024**, *25*, 101793. [\[CrossRef\]](#)

32. Adarme, O.F.H.; Baêta, B.E.L.; Lima, D.R.S.; Gurgel, L.V.A.; de Aquino, S.F. Methane and hydrogen production from anaerobic digestion of soluble fraction obtained by sugarcane bagasse ozonation. *Ind. Crops Prod.* **2017**, *109*, 288–299. [\[CrossRef\]](#)

33. Braga, J.K.; Soares, L.A.; Motteran, F.; Sakamoto, I.K.; Varesche, M.B.A. Effect of 2-bromoethanesulfonate on anaerobic consortium to enhance hydrogen production utilizing sugarcane bagasse. *Int. J. Hydrogen Energy* **2016**, *41*, 22812–22823. [\[CrossRef\]](#)

34. Tondro, H.; Musivand, S.; Zilouei, H.; Bazarganipour, M.; Zargoosh, K. Biological production of hydrogen and acetone- butanol-ethanol from sugarcane bagasse and rice straw using co-culture of *Enterobacter aerogenes* and *Clostridium acetobutylicum*. *Biomass Bioenergy* **2020**, *142*, 105818. [\[CrossRef\]](#)

35. Bu, J.; Wang, Y.-T.; Deng, M.-C.; Zhu, M.-J. Enhanced enzymatic hydrolysis and hydrogen production of sugarcane bagasse pretreated by peroxyformic acid. *Bioresour. Technol.* **2021**, *326*, 124751. [\[CrossRef\]](#)

36. Chen, S.-J.; Chen, X.; Hu, B.-B.; Wei, M.-Y.; Zhu, M.-J. Efficient hydrogen production from sugarcane bagasse and food waste by thermophilic clostridiales consortium and Fe–Mn impregnated biochars. *Renew. Energy* **2023**, *211*, 166–178. [\[CrossRef\]](#)

37. Dharmaraja, J.; Shobana, S.; Arvindnarayanan, S.; Francis, R.R.; Jeyakumar, R.B.; Saratale, R.G.; Ashokkumar, V.; Bhatia, S.K.; Kumar, V.; Kumar, G. Lignocellulosic biomass conversion via greener pretreatment methods towards biorefinery applications. *Bioresour. Technol.* **2023**, *369*, 128328. [\[CrossRef\]](#)

38. Vasconcelos, M.H.; Mendes, F.M.; Ramos, L.; Dias, M.O.S.; Bonomi, A.; Jesus, C.D.F.; Watanabe, M.D.B.; Junqueira, T.L.; Milagres, A.M.F.; Ferraz, A.; et al. Techno-economic assessment of bioenergy and biofuel production in integrated sugarcane biorefinery: Identification of technological bottlenecks and economic feasibility of dilute acid pretreatment. *Energy* **2020**, *199*, 117422. [\[CrossRef\]](#)

39. Betancur, G.; Pereira, N., Jr. Sugar cane bagasse as feedstock for second generation ethanol production. Part I: Diluted acid pretreatment optimization. *Electron. J. Biotechnol.* **2010**, *13*, 10–11. [\[CrossRef\]](#)

40. Maintinguier, S.I.; Fernandes, B.S.; Duarte, I.C.S.; Saavedra, N.K.; Adorno, M.A.T.; Varesche, M.B. Fermentative hydrogen production by microbial consortium. *Int. J. Hydrogen Energy* **2008**, *33*, 4309–4317. [\[CrossRef\]](#)

41. Eaton, A.D.; Franson, M.A.H.; Association, A.P.H.; Association, A.W.W.; Federation, W.E. *Standard Methods for the Examination of Water and Wastewater*; American Public Health Association: Washington, DC, USA, 2005.

42. DuBois, M.; Gilles, K.A.; Hamilton, J.K.; Rebers, P.T.; Smith, F. Colorimetric Method for Determination of Sugars and Related Substances. *Anal. Chem.* **1956**, *28*, 350–356. [\[CrossRef\]](#)

43. Mockaitis, G.; Rodrigues, J.A.D.; Foresti, E.; Zaiat, M. Toxic effects of cadmium (Cd2+) on anaerobic biomass: Kinetic and metabolic implications. *J. Environ. Manag.* **2012**, *106*, 75–84. [\[CrossRef\]](#)

44. Peixoto, G.; Saavedra, N.K.; Varesche, M.B.A.; Zaiat, M. Hydrogen production from soft-drink wastewater in an upflow anaerobic packed-bed reactor. *Int. J. Hydrogen Energy* **2011**, *36*, 8953–8966. [\[CrossRef\]](#)

45. Zheng, H.-S.; Guo, W.-Q.; Yang, S.-S.; Feng, X.-C.; Du, J.-S.; Zhou, X.-J.; Chang, J.-S.; Ren, N.-Q. Thermophilic hydrogen production from sludge pretreated by thermophilic bacteria: Analysis of the advantages of microbial community and metabolism. *Bioresour. Technol.* **2014**, *172*, 433–437. [\[CrossRef\]](#)

46. Coelho, N.M.G.; Droste, R.L.; Kennedy, K.J. Evaluation of continuous mesophilic, thermophilic and temperature phased anaerobic digestion of microwaved activated sludge. *Water Res.* **2011**, *45*, 2822–2834. [\[CrossRef\]](#)

47. Zhang, T.; Liu, H.; Fang, H.H.P. Biohydrogen production from starch in wastewater under thermophilic condition. *J. Environ. Manag.* **2003**, *69*, 149–156. [\[CrossRef\]](#) [\[PubMed\]](#)

48. Karadag, D. Anaerobic H2 production at elevated temperature (60 °C) by enriched mixed consortia from mesophilic sources. *Int. J. Hydrogen Energy* **2011**, *36*, 458–465. [\[CrossRef\]](#)

49. Mamimin, C.; Prasertsan, P. Effect of temperature and initial pH on biohydrogen production from palm oil mill effluent: Long-term evaluation and microbial community analysis. *Electron. J. Biotechnol.* **2011**, *14*, 9.

50. Puhakka, J.A.; Karadag, D.; Nissilä, M.E. Comparison of mesophilic and thermophilic anaerobic hydrogen production by hot spring enrichment culture. *Int. J. Hydrogen Energy* **2012**, *37*, 16453–16459. [\[CrossRef\]](#)

51. Łukajtis, R.; Hołowacz, I.; Kucharska, K.; Glinka, M.; Rybarczyk, P.; Przyjazny, A.; Kamiński, M. Hydrogen production from biomass using dark fermentation. *Renew. Sustain. Energy Rev.* **2018**, *91*, 665–694. [\[CrossRef\]](#)

52. Thi Nguyen, M.-L.; Hung, P.-C.; Vo, T.-P.; Lay, C.-H.; Lin, C.-Y. Effect of food to microorganisms (F/M) ratio on biohythane production via single-stage dark fermentation. *Int. J. Hydrogen Energy* **2021**, *46*, 11313–11324. [\[CrossRef\]](#)

53. Barua, V.B.; Kalamdhad, A.S. Anaerobic biodegradability test of water hyacinth after microbial pretreatment to optimise the ideal F/M ratio. *Fuel* **2018**, *217*, 91–97. [\[CrossRef\]](#)

54. Abdullah, B.; Muhammad, S.A.F.A.S.; Shokravi, Z.; Ismail, S.; Kassim, K.A.; Mahmood, A.N.; Aziz, M.M.A. Fourth generation biofuel: A review on risks and mitigation strategies. *Renew. Sustain. Energy Rev.* **2019**, *107*, 37–50. [\[CrossRef\]](#)

55. Saidi, R.; Liebgott, P.P.; Hamdi, M.; Auria, R.; Bouallagui, H. Enhancement of fermentative hydrogen production by *Thermotoga maritima* through hyperthermophilic anaerobic co-digestion of fruit-vegetable and fish wastes. *Int. J. Hydrogen Energy* **2018**, *43*, 23168–23177. [\[CrossRef\]](#)

56. Wang, B.; Li, Y.; Ren, N. Biohydrogen from molasses with ethanol-type fermentation: Effect of hydraulic retention time. *Int. J. Hydrogen Energy* **2013**, *38*, 4361–4367. [\[CrossRef\]](#)

57. Guo, W.-Q.; Ren, N.-Q.; Wang, X.-J.; Xiang, W.-S.; Meng, Z.-H.; Ding, J.; Qu, Y.-Y.; Zhang, L.-S. Biohydrogen production from ethanol-type fermentation of molasses in an expanded granular sludge bed (EGSB) reactor. *Int. J. Hydrogen Energy* **2008**, *33*, 4981–4988. [\[CrossRef\]](#)

58. Ren, N.; Li, J.; Li, B.; Wang, Y.; Liu, S. Biohydrogen production from molasses by anaerobic fermentation with a pilot-scale bioreactor system. *Int. J. Hydrogen Energy* **2006**, *31*, 2147–2157. [\[CrossRef\]](#)

59. Hawkes, F.R.; Hussy, I.; Kyazze, G.; Dinsdale, R.; Hawkes, D.L. Continuous dark fermentative hydrogen production by mesophilic microflora: Principles and progress. *Int. J. Hydrogen Energy* **2007**, *32*, 172–184. [\[CrossRef\]](#)

60. Chen, C.-C.; Sen, B.; Chuang, Y.-S.; Tsai, C.-J.; Lay, C.-H. Effect of effluent recycle ratio in a continuous anaerobic biohydrogen production system. *J. Clean. Prod.* **2012**, *32*, 236–243. [\[CrossRef\]](#)

61. Tawfik, A.; El-Qelish, M. Continuous hydrogen production from co-digestion of municipal food waste and kitchen wastewater in mesophilic anaerobic baffled reactor. *Bioresour. Technol.* **2012**, *114*, 270–274. [\[CrossRef\]](#) [\[PubMed\]](#)

62. Kyazze, G.; Martinez-Perez, N.; Dinsdale, R.; Premier, G.C.; Hawkes, F.R.; Guwy, A.J.; Hawkes, D.L. Influence of substrate concentration on the stability and yield of continuous biohydrogen production. *Biotechnol. Bioeng.* **2006**, *93*, 971–979. [\[CrossRef\]](#)

63. Kim, S.-H.; Han, S.-K.; Shin, H.-S. Effect of substrate concentration on hydrogen production and 16S rDNA-based analysis of the microbial community in a continuous fermenter. *Process Biochem.* **2006**, *41*, 199–207. [\[CrossRef\]](#)

64. Chen, C.-C.; Chen, H.-P.; Wu, J.-H.; Lin, C.-Y. Fermentative hydrogen production at high sulfate concentration. *Int. J. Hydrogen Energy* **2008**, *33*, 1573–1578. [\[CrossRef\]](#)

65. Hussy, I.; Hawkes, F.R.; Dinsdale, R.; Hawkes, D.L. Continuous Fermentative Hydrogen Production from a Wheat Starch Co-Product by Mixed Microflora. *Biotechnol. Bioeng.* **2003**, *84*, 619–626. [\[CrossRef\]](#)

66. van Niel, E.; Claassen, P.; Stams, A. Substrate and product inhibition of hydrogen production by the extreme thermophile, *Caldicellulosiruptor saccharolyticus*. *Biotechnol. Bioeng.* **2003**, *81*, 255–262. [\[CrossRef\]](#)

67. Kádár, Z.; de Vrie, T.; van Noorden, G.E.; Budde, M.A.; Szengyel, Z.; Réczy, K.; Claassen, P.A. Yields from glucose, xylose, and paper sludge hydrolysate during hydrogen production by the extreme thermophile *Caldicellulosiruptor saccharolyticus*. *Appl. Biochem. Biotechnol.* **2004**, *114*, 497–508. [\[CrossRef\]](#)

68. Abdel-Rahman, M.A.; Xiao, Y.; Tashiro, Y.; Wang, Y.; Zendo, T.; Sakai, K.; Sonomoto, K. Fed-batch fermentation for enhanced lactic acid production from glucose/xylose mixture without carbon catabolite repression. *J. Biosci. Bioeng.* **2015**, *119*, 153–158. [\[CrossRef\]](#) [\[PubMed\]](#)

69. Sakai, K.; Ezaki, Y. Open L-lactic acid fermentation of food refuse using thermophilic *Bacillus coagulans* and fluorescence in situ hybridization analysis of microflora. *J. Biosci. Bioeng.* **2006**, *101*, 457–463. [\[CrossRef\]](#) [\[PubMed\]](#)

70. Heriban, V.; ŠTurdík, E.; Zalibera, L.; Matuš, P. Process and metabolic characteristics of *Bacillus coagulans* as lactic acid producer. *Lett. Appl. Microbiol.* **2008**, *16*, 243–246. [\[CrossRef\]](#)

71. Ye, L.; Zhou, X.; Hudari, M.S.B.; Li, Z.; Wu, J.C. Highly efficient production of l-lactic acid from xylose by newly isolated *Bacillus coagulans* C106. *Bioresour. Technol.* **2013**, *132*, 38–44. [\[CrossRef\]](#)

72. Tanaka, K.; Komiya, A.; Sonomoto, K.; Ishizaki, A.; Hall, S.; Stanbury, P. Two different pathways for D-xylose metabolism and the effect of xylose concentration on the yield coefficient of L-lactate in mixed-acid fermentation by the lactic acid bacterium *Lactococcus lactis* IO-1. *Appl. Microbiol. Biotechnol.* **2002**, *60*, 160–167. [\[CrossRef\]](#)

73. Zhang, K.; Woodruff, A.; Xiong, M.; Zhou, J.; Dhande, Y. A Synthetic Metabolic Pathway for Production of the Platform Chemical Isobutyric Acid. *ChemSusChem* **2011**, *4*, 1068–1070. [\[CrossRef\]](#)

74. Ding, H.-B.; Tan, G.-Y.A.; Wang, J.-Y. Caproate formation in mixed-culture fermentative hydrogen production. *Bioresour. Technol.* **2010**, *101*, 9550–9559. [\[CrossRef\]](#) [\[PubMed\]](#)

75. Galbally, I.E.; Kirstine, W. The Production of Methanol by Flowering Plants and the Global Cycle of Methanol. *J. Atmos. Chem.* **2002**, *43*, 195–229. [\[CrossRef\]](#)

76. Pegoraro, J.; Salem, N.F.M.; Andreazzi, M.A.; Dos Santos, J.M.G. *Uso de Glicerina na Alimentação Animal*; VI Mostra Interna de Trabalhos de Iniciação Científica: Maringá, Brazil, 2011.

77. Ohimain, E.I. Methanol contamination in traditionally fermented alcoholic beverages: The microbial dimension. *Springerplus* **2016**, *5*, 1607. [\[CrossRef\]](#)

78. Hamacher, T.; Becker, J.; Gárdonyi, M.; Hahn-Hägerdal, B.; Boles, E. Characterization of the xylose-transporting properties of yeast hexose transporters and their influence on xylose utilization. *Microbiology* **2002**, *148*, 2783–2788. [\[CrossRef\]](#) [\[PubMed\]](#)

79. Prakasham, R.S.; Brahmaiah, P.; Sathish, T.; Sambasiva Rao, K.R.S. Fermentative biohydrogen production by mixed anaerobic consortia: Impact of glucose to xylose ratio. *Int. J. Hydrogen Energy* **2009**, *34*, 9354–9361. [\[CrossRef\]](#)

80. Temudo, M.F.; Mato, T.; Kleerebezem, R.; van Loosdrecht, M.C.M. Xylose anaerobic conversion by open-mixed cultures. *Appl. Microbiol. Biotechnol.* **2009**, *82*, 231–239. [\[CrossRef\]](#) [\[PubMed\]](#)

81. Fangkum, A.; Reungsang, A. Biohydrogen production from sugarcane bagasse hydrolysate by elephant dung: Effects of initial pH and substrate concentration. *Int. J. Hydrogen Energy* **2011**, *36*, 8687–8696. [\[CrossRef\]](#)

82. Pateraki, C.; Almqvist, H.; Ladakas, D.; Lidén, G.; Koutinas, A.A.; Vlysidis, A. Modelling succinic acid fermentation using a xylose based substrate. *Biochem. Eng. J.* **2016**, *114*, 26–41. [\[CrossRef\]](#)

83. Tomás, A.; Karakashev, D.; Angelidaki, I. Effect of xylose and nutrients concentration on ethanol production by a newly isolated extreme thermophilic *Thermoanaerobacter* sp. In Proceedings of the 12th World Congress on Anaerobic Digestion, Guadalajara, Mexico, 31 October–4 November 2010.

84. Palmqvist, E.; Hahn-Hägerdal, B. Fermentation of lignocellulosic hydrolysates. II: Inhibitors and mechanisms of inhibition. *Bioresour. Technol.* **2000**, *74*, 25–33. [\[CrossRef\]](#)

85. Bundhoo, M.A.Z.; Mohee, R. Inhibition of dark fermentative bio-hydrogen production: A review. *Int. J. Hydrogen Energy* **2016**, *41*, 6713–6733. [\[CrossRef\]](#)

86. Quéméneur, M.; Hamelin, J.; Barakat, A.; Steyer, J.-P.; Carrère, H.; Trably, E. Inhibition of fermentative hydrogen production by lignocellulose-derived compounds in mixed cultures. *Int. J. Hydrogen Energy* **2012**, *37*, 3150–3159. [\[CrossRef\]](#)

87. Cao, G.-L.; Ren, N.-Q.; Wang, A.-J.; Guo, W.-Q.; Xu, J.-F.; Liu, B.-F. Effect of lignocellulose-derived inhibitors on growth and hydrogen production by *Thermoanaerobacterium thermosaccharolyticum* W16. *Int. J. Hydrogen Energy* **2010**, *35*, 13475–13480. [\[CrossRef\]](#)

88. Akobi, C.; Hafez, H.; Nakhla, G. The impact of furfural concentrations and substrate-to-biomass ratios on biological hydrogen production from synthetic lignocellulosic hydrolysate using mesophilic anaerobic digester sludge. *Bioresour. Technol.* **2016**, *221*, 598–606. [\[CrossRef\]](#) [\[PubMed\]](#)

89. Veeravalli, S.S.; Chaganti, S.R.; Lalman, J.A.; Heath, D.D. Effect of furans and linoleic acid on hydrogen production. *Int. J. Hydrogen Energy* **2013**, *38*, 12283–12293. [\[CrossRef\]](#)

90. Aguilar, R.; Ramírez, J.A.; Garrote, G.; Vázquez, M. Kinetic study of the acid hydrolysis of sugar cane bagasse. *J. Food Eng.* **2002**, *55*, 309–318. [\[CrossRef\]](#)

91. Wang, B.; Wan, W.; Wang, J. Inhibitory effect of ethanol, acetic acid, propionic acid and butyric acid on fermentative hydrogen production. *Int. J. Hydrogen Energy* **2008**, *33*, 7013–7019. [\[CrossRef\]](#)

92. Wang, Y.; Zhao, Q.-B.; Mu, Y.; Yu, H.-Q.; Harada, H.; Li, Y.-Y. Biohydrogen production with mixed anaerobic cultures in the presence of high-concentration acetate. *Int. J. Hydrogen Energy* **2008**, *33*, 1164–1171. [\[CrossRef\]](#)

93. Chin, H.-L.; Chen, Z.-S.; Chou, C.P. Fedbatch Operation Using *Clostridium acetobutylicum* Suspension Culture as Biocatalyst for Enhancing Hydrogen Production. *Biotechnol. Prog.* **2003**, *19*, 383–388. [\[CrossRef\]](#)

94. Logan, B. Inhibition of Bio-Hydrogen Production by Un-Dissociated Acetic and Butyric Acids. *Environ. Sci. Technol.* **2005**, *39*, 9351–9356. [\[CrossRef\]](#)

95. Mizuno, O.; Li, Y.Y.; Noike, T. The behavior of sulfate-reducing bacteria in acidogenic phase of anaerobic digestion. *Water Res.* **1998**, *32*, 1626–1634. [\[CrossRef\]](#)

96. Lin, C.-Y.; Chen, H.-P. Sulfate effect on fermentative hydrogen production using anaerobic mixed microflora. *Int. J. Hydrogen Energy* **2006**, *31*, 953–960. [\[CrossRef\]](#)

Disclaimer/Publisher's Note: The statements, opinions and data contained in all publications are solely those of the individual author(s) and contributor(s) and not of MDPI and/or the editor(s). MDPI and/or the editor(s) disclaim responsibility for any injury to people or property resulting from any ideas, methods, instructions or products referred to in the content.